

Initial Results of Accelerated Stress Testing on Single-Channel and Multichannel Drivers

Solid-State Lighting Technology Area

February 2018
(Revised June 2018)

RTI Project Number
0215939.001.001

Accelerated Stress Testing on Single-Channel and Multichannel Drivers*

**February 2018
(Revised June 2018)**

Prepared for

Client Name: U.S. Department of Energy
3610 Collins Ferry Road
Morgantown, WV 26505

Prepared by

**RTI Author(s): Lynn Davis, Kelley Rountree, Karmann Mills,
and Praneet Athalye**
RTI International
3040 E. Cornwallis Road
Research Triangle Park, NC 27709

* This report has been revised from the original version submitted to the U.S. Department of Energy, Office of Energy Efficiency and Renewable Energy (EERE).

Acknowledgments

This material is based upon work supported by the Department of Energy, Office of Energy Efficiency and Renewable Energy (EERE), under Award Number DE-FE0025912.

This work benefitted greatly from many discussions of driver performance with Terry Clark and Aaron Smith of Finelite, Inc. and Warren Weeks of Hubbell Lighting Inc. The donation of samples by both Finelite and Hubbell Lighting and the contributions of both companies in analyzing the drivers are also gratefully acknowledged.

Disclaimer

This report was prepared as an account of work sponsored by an agency of the United States Government. Neither the United States Government nor any agency thereof, nor any of their employees, makes any warranty, express or implied, or assumes any legal liability or responsibility for the accuracy, completeness, or usefulness of any information, apparatus, product, or process disclosed, or represents that its use would not infringe privately owned rights. Reference herein to any specific commercial product, process, or service by trade name, trademark, manufacturer, or otherwise does not necessarily constitute or imply its endorsement, recommendation, or favoring by the United States Government or any agency thereof. The views and opinions of authors expressed herein do not necessarily state or reflect those of the United States Government or any agency thereof.

List of Acronyms

ac	alternating current
AST	accelerated stress testing
CALiPER	Commercially Available LED Product Evaluation and Reporting
CCT	correlated color temperature
CRI	color rendering index
CSM	Chromaticity Shift Mode
dc	direct current
DMX	digital multiplex
DOE	U.S. Department of Energy
DUT	device under test
HAST	highly accelerated stress testing
IC	integrated circuit
IP	Ingress Protection
LED	light-emitting diode
LLC	inductor inductor capacitor
MOSFET	metal-oxide-semiconductor field-effect transistor
MOV	metal oxide varistor
PCB	printed circuit board
pcLED	phosphor-converted LED
PF	power factor
PFC	power factor correction
PWM	pulse width modulation
RTOL	room temperature operational lifetime
SIMO	single-inductor multiple-output
SMPS	switched mode power supply
SSL	solid-state lighting
TC	thermocouple
THD	total harmonic distortion
TWL	tunable-white lighting

Executive Summary

The primary function of the drivers used in solid-state lighting (SSL) luminaires is to efficiently convert the power from the electrical mains into a form that can be used to operate the light-emitting diodes (LEDs). This function is achieved through a series of electrical circuits contained in the driver that first convert the input alternating current (ac) into an intermediate direct current (dc) signal and finally into the output dc signal. Because SSL devices are generally expected to have greater reliability than their conventional lighting counterparts, the reliability of each component of the lighting system, including the driver, must be considered carefully. The reliability of SSL drivers is dependent upon the combined reliability of all the electrical circuits in the driver. The failure of any component in a driver may impact the performance of that driver, including by changing the output dc power waveform, altering the power factor (PF) or efficiency of the device, and introducing harmonic distortion into the branch electrical circuit. The cumulative effects of aging that occur within the driver can lead to the failure of the entire SSL luminaire, resulting in abrupt, lights-out failures; reduced luminous flux failures; and even excess flicker failures.

This report is the first in a series of studies on accelerated stress testing (AST) of drivers used for SSL luminaires, such as downlights, troffers, and streetlights. A representative group of two-stage commercial driver products was exposed to an AST environment consisting of 75°C and 75% relative humidity (7575). These drivers were a mix of single-channel drivers (i.e., a single output current for one LED primary) and multichannel drivers (i.e., separate output currents for multiple LED primaries). This AST environment was chosen because previous testing on downlights with integrated drivers demonstrated that 38% of the sample population failed in less than 2,500 hours of testing using this method. In addition to AST test results, the performance of an SSL downlight product incorporating an integrated, multichannel driver during extended room temperature operational life (RTOL) testing is also reported. A battery of measurements was used to evaluate these products during accelerated testing, including full electrical characterization (i.e., power consumption, PF, total harmonic distortion [THD], and inrush current) and photometric characterization of external LED loads attached to the drivers (i.e., flicker performance and lumen maintenance).

LEDs are imparting new capabilities to SSLs, including the ability to incorporate multiple LED primaries into a light source and to provide illumination that can be tuned over a range of correlated color temperatures (CCTs). This capability is termed tunable-white lighting (TWL) and can have a number of advantages in schools, health care facilities, and offices. Products providing white light that can be tuned over a range of CCT values require the ability to control the current delivered to each LED primary independently. This can be achieved by either assigning individual, single-channel drivers to each LED primary or using one driver with separate power control channels for each LED primary (i.e., a multichannel driver). Each of these approaches is evaluated in this study in terms of its potential reliability, system complexity, and cost.

AST testing of the single-channel and multichannel drivers demonstrated that most of the tested products exhibited minimal performance degradation after 2,500 hours of exposure to the 7575 environment. Of the 12 samples tested to date, only two have failed, corresponding to a failure rate of 17%. This value is slightly less than half that found in previous testing for 6" downlights and suggests that these products have good reliability and robustness. The two failed devices were from the same product, and the root cause of failure was traced to film capacitors and the metal-oxide-semiconducting field-effect transistor (MOSFET) in the power factor correction (PFC) stage. Failure was shown to occur abruptly, likely because of the cumulative effects of degradation, and was not solely attributable to one-time events, such as power being applied. The other devices exhibited no significant changes in either their electrical or photometric properties, even after 2,500 hours of exposure to the harsh AST environment.

The findings in this report demonstrate that many of the drivers used in SSL devices are highly robust and can withstand extreme conditions for extended periods with minimal changes in key electrical performance parameters, such as power output, PF, and THD. In addition, virtually no change in photometric properties occurred after 2,500 hours of 7575. This finding is especially important because photometric changes (e.g.,

luminous flux, flicker, and chromaticity) may be noticeable to the end-user and building managers, whereas electrical changes are less likely to be noticed. The observation of minimal changes in both the electrical and photometric performance of SSL systems incorporating these drivers increases the confidence that many SSL devices, when installed properly, can provide expected energy savings over the lifetime of the product and meet expected return-on-investment goals.

Table of Contents

Acknowledgments	iii
List of Acronyms	v
Executive Summary	vi
1 Background Information	1
1.1 Introduction and Applications of Single-Channel and Multichannel Drivers	1
1.1.1 Basics of Driver Structure	1
1.1.2 LED Properties.....	5
1.2 Driver Configurations and Common Use	7
1.2.1 Basics of Driver Structure	7
1.2.2 Two-Stage Multichannel Drivers	8
2 Test Samples	11
3 Experimental Procedures	12
3.1 Accelerated Stress Tests	12
3.2 RTOL Testing.....	13
3.3 Accelerated Testing Methods	13
3.4 Measurement Methods	13
3.4.1 Temperature	13
3.4.2 Electrical	14
3.4.3 Photometric	15
4 Findings	16
4.1 Cree LR6 Downlight	16
4.2 Single-Channel Drivers	21
4.3 Multichannel Drivers.....	24
5 Conclusions	32
Appendix A	35

List of Figures

Figure 1–1. Block diagram of the major functions of many drivers used with SSL devices.	1
Figure 1–2. Circuit 1 components of select SSL drivers.....	2
Figure 1–3. Buck dc output stage for a multichannel driver.	3
Figure 1–4. Pictures of single-stage drivers used in SSL downlights, PAR38 lamps, and A19 lamps.	4
Figure 1–5. Two-stage drivers used in SSL troffers and downlights.....	5
Figure 1–6. Examples of LED modules comprising multiple LED assemblies for use in TWL devices.	6
Figure 1–7. Schematic of a two-stage single-channel driver.....	8
Figure 1–8. Schematic of multiple two-stage single-channel drivers combined with a user interface (e.g., dimming control) in a TWL system with two LED primaries.	8
Figure 1–9. Schematic representation of a two-stage dual-channel driver for operating a TWL system with two LED primaries.	9
Figure 1–10. Detailed schematic of the buck converter often used to control the dc output to the LEDs in a two-stage multichannel driver.	9
Figure 1–11. Schematic illustration of the operations of a TWL with two LED primaries.	10
Figure 3–1. Configuration of the DUTs during AST exposure and the connecting wires to the ac source and the LED loads.	12
Figure 3–2. Exterior of the test chamber showing the LED loads on top of the chamber and the connecting wires to the DUTs.....	13
Figure 3–3. Temperature measurement of an integrated IC and MOSFET package on a multichannel driver undergoing AST.....	14
Figure 4–1. LED light source and driver for the Cree LR6 downlight.	16
Figure 4–2. Luminous flux maintenance of three Cree LR6 luminaires subjected to the Hammer test [8].....	17
Figure 4–3. Change in the chromaticity coordinates of Cree LR6 luminaires during the Hammer Test.	18
Figure 4–4. Luminous flux maintenance of the Cree LR6 samples during RTOL testing.	19
Figure 4–5. Chromaticity shift of the Cree LR6 samples during RTOL testing.	19
Figure 4–6. Flicker profile of the control Cree LR6.	20
Figure 4–7. Photometric flicker waveform of an LR6 device (Sample 1) that failed during RTOL testing.....	21
Figure 4–8. Output power and driver efficiency as a function of input voltage for DUT-S2.....	23
Figure 4–9. Output power and driver efficiency as a function of the input power for a DUT-S2	

sample	23
Figure 4–10. 0–10-V dimming characteristics of DUT-S3 before and after 7575 exposure.....	24
Figure 4–11. TC profile of the DUT-M1 sample in 7575 when failure occurred	26
Figure 4–12. Inrush peak current comparisons of the control and sample DUT-M2 devices as a function of dimming percentage, showing higher inrush currents on the control device.....	27
Figure 4–13. PF comparison of the control and sample DUT-M2 devices as a function of the dimming percentage	28
Figure 4–14. Comparison of the photometric flicker waveform, at 1% dimming, between a DUT-M2 sample after 2,500 hours of 7575 exposure and a control device.	29
Figure 4–15. PF comparison of the control and sample DUT-M3 devices as a function of the dimming percentage	30
Figure 4–16. Comparison of the photometric flicker waveform, at 1% dimming, between a DUT-M3 sample after 2,500 hours of 7575 exposure and a control device.	31

List of Tables

Table 3-1. Photometric properties measured during this study with the GigaHertz-Optik BTS-256-EF.^a	15
Table 4-1. Comparison of the photometric flicker parameters of the failed RTOL and control LR6 samples.....	21
Table 4-2. Manufacturer’s specifications for the multichannel drivers examined in this study.....	22
Table 4-3. Manufacturer’s specifications for the multichannel drivers examined in this study.....	25
Table 4-4. Change in the electrical properties of a DUT-M1 sample before and after 7575 exposure.	26
Table 4-5. Efficiencies of the control and sample 1 (post 2,500 hours of 7575 exposure) DUT-M2 drivers at various dimming levels.....	28
Table 4-6. Efficiencies of the control and sample 1 (post 2,500 hours of 7575 exposure) DUT-M3 drivers at various dimming levels.....	30
Table Appendix A-1. Identifying information for the samples included in this report	35

1 Background Information

1.1 Introduction and Applications of Single-Channel and Multichannel Drivers

1.1.1 Basics of Driver Structure

Drivers used to power solid-state lighting (SSL) lamps and luminaires are complicated devices comprising multiple electrical circuits, each designed for a specific purpose. The intent of this collection of electrical circuits is to efficiently convert power from the electrical mains into a form that can operate SSL devices. A block diagram showing the relationship among some of the major circuits in an SSL driver is shown in **Figure 1-1**. Additional circuitry for functions such as dimming and wireless access may be included in some drivers. At a minimum, the circuits contained in the SSL driver are designed to work cohesively to achieve four main functions:

1. **CIRCUIT 1:** Condition the alternating current (ac) input provided by the electrical mains and provide surge suppression;
2. **CIRCUIT 2:** Convert the ac input into an intermediate direct current (dc) feed, usually through the process of rectification;
3. **CIRCUIT 3:** Provide power factor correction (PFC) to the dc feed to promote high power factor (PF) and low total harmonic distortion (THD); and
4. **CIRCUIT 4:** Convert the post-rectification dc feed to the appropriate dc voltage and current to drive the light-emitting diode (LED) arrays.

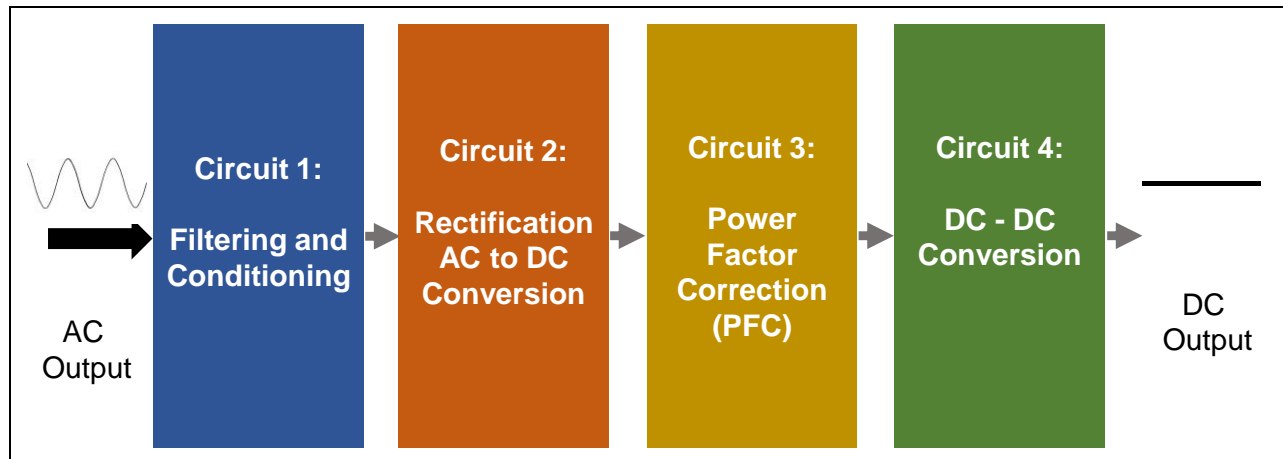


Figure 1-1. Block diagram of the major functions of many drivers used with SSL devices.

In Circuit 1 of the LED driver, in some cases, the electrical power from the ac mains can be filtered by capacitors and inductors to minimize the effects of transients, surges, and sags in the electrical mains. In addition, capacitors and inductors can be used to form an electromagnetic interference filter to prevent harmonics created during the power conversion process from being introduced onto the ac line. Some of the capacitors used in the suppression and filter circuits bridge across the electrical inputs (i.e., X capacitors), whereas other capacitors connect the mains to ground (i.e., Y capacitors). Often, these capacitors are film capacitors because of their high reliability and dielectric strength. Two additional components that are often found in Circuit 1 are the metal oxide varistor (MOV), which provides surge suppression, and a fuse, which provides additional circuit protection. The ac output from Circuit 1 is typically fed into a bridge diode to rectify the ac voltage and begin the conversion to dc. Examples of typical Circuit 1 layouts used in SSL drivers are shown in **Figure 1-2**.

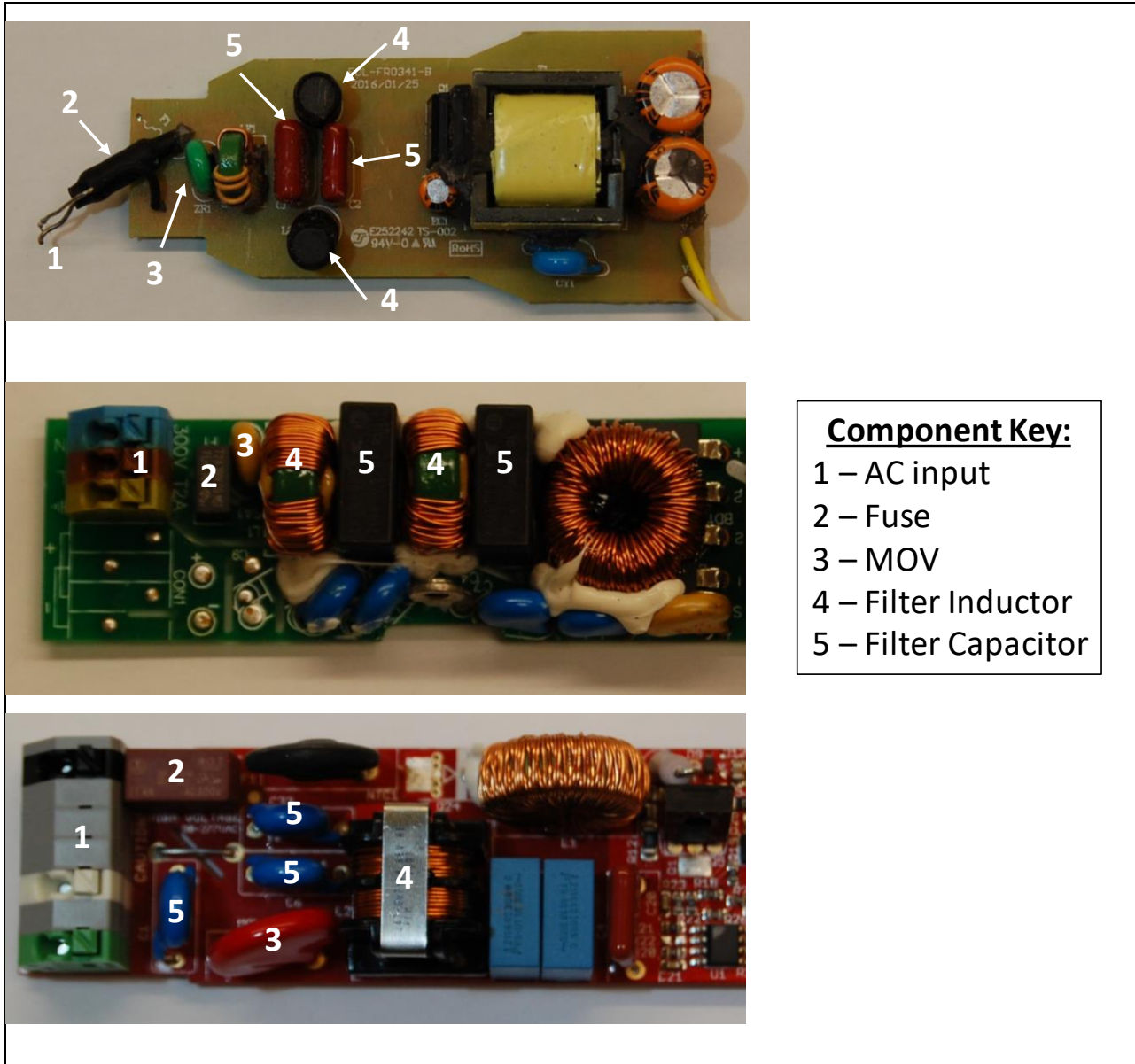


Figure 1-2. Circuit 1 components of select SSL drivers.

While the output from the rectification process (i.e., Circuit 2) is an intermediate dc signal, there is usually a significant amount of ripple that, if it is not removed, can lead to undesirable side effects, such as excessive photometric flicker, in the final output voltage. Ripple in the dc signal can be eliminated with a filtering process that involves additional capacitors and inductors placed after the rectifier. Unfortunately, this process causes the current and voltage to become out of phase, which can lead to further issues with PF and harmonic distortion, if not corrected. Circuit 3 provides the corrective circuitry that not only reduces ripple in the intermediate dc signal but also provides PFC and reduces THD.

The PF of a circuit depends on the displacement between the voltage and current waveforms and the amount of THD. This relationship is shown in **Equation 1**.

$$Power\ Factor\ (PF) = \cos(\theta_v - \theta_i) \sqrt{\frac{1}{1+THD}} \quad (\text{Equation 1})$$

where θ_v is the voltage phase, and θ_i is the current phase. The phase of the current produced by an electrical circuit (i.e., θ_i) depends on the load. For resistive loads, the current and voltage are in phase; in contrast, the current lags the voltage in inductive loads but leads the voltage in capacitive loads. Ideally, the PF should be close to one, which indicates not only that the current and voltage are in phase but also that the distortion caused by the load is low. Alternatively, PF can be viewed as the power consumed by the load divided by the power delivered. When the PF is not close to one, the delivered power is not completely consumed by the load, and the remaining power circulates back and forth between the source and the load, causing additional losses.

The final stage (i.e., Circuit 4) of a typical SSL driver is a dc–dc conversion stage in which the output dc current (i.e., that delivered to the LEDs) is set, effectively determining the LED string voltage. Often, a capacitor is used across the input voltage rails between Circuit 3 and Circuit 4 to maintain a constant dc input voltage for Circuit 4. In general, dc–dc conversion can be accomplished using passive circuits, such as voltage dividers (i.e., passive conversion), or by rapidly switching the power level (i.e., switched-mode conversion). The use of a dissipative resistor load in passive converters lowers their efficiency and produces a significant amount of waste heat. Consequently, the vast majority of dc–dc converters in SSL drivers are switched-mode power supplies (SMPSs) that control output power levels through a high-frequency switching cycle. A significant advantage of the SMPS architecture is that it is more efficient than linear converters. The core of an SMPS device is a semiconductor switch, such as a metal-oxide-semiconductor field-effect transistor (MOSFET) that is switched at a duty cycle set by a controller integrated circuit (IC). Because the power delivered by the MOSFET ultimately determines the illuminance produced by the LED load, very accurate control of the switching waveform is necessary. Degradation of the driver circuit can lead to changes in this waveform and alterations in the properties of the emitted light (e.g., luminous flux or flicker) produced by the SSL device. In many instances, a MOSFET is combined with additional circuitry to provide energy storage during the off cycle of the MOSFET switch. For example, an inductor (in series with the LED load) paired with a capacitor (parallel to the LED load) are commonly used to provide energy storage in SSL devices; this is a classic buck converter topology. An example of this type of layout is given in **Figure 1-3**.

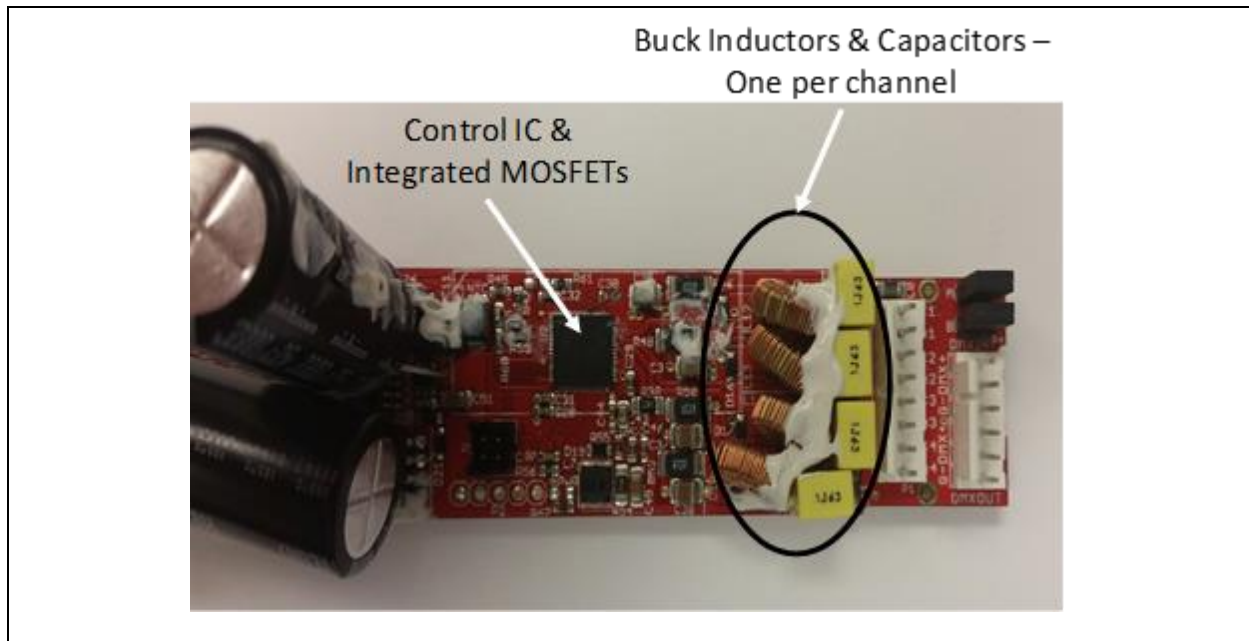


Figure 1-3. Buck dc output stage for a multichannel driver.

Depending upon the voltage necessary to drive the LED loads, various driver topologies can be used in the dc–dc converter, including buck, boost, and flyback converters [1, 2]. Buck converters are low-cost voltage step-down power sources, and boost converters are low-cost voltage step-up converters. Flyback converters are a

type of buck-boost device and provide either voltage step-up or step-down, depending upon the configuration, in addition to electrical isolation.

SSL drivers are designed to maximize the efficiency of converting ac power to dc power while minimizing THD and photometric flicker. Driver efficiency is impacted by the cumulative efficiencies of all circuits shown in Figure 1-1, although the dc–dc conversion stage plays a significant role in overall device efficiency. For SMPS devices, the primary source of inefficiency is switching losses, which can be minimized by proper design and component selection. Aging-related degradation of the components of these circuits or the feed circuits that provide power can cause the performance of the SSL device to fall outside of end-users' expectations, possibly to the point of being classified as a failed device. THD and photometric flicker are primarily impacted by the PFC and dc–dc conversion stages, respectively.

Depending upon the space requirements and performance specifications of the SSL driver, the PFC and dc–dc conversion stages can be optimized together or separately. Combining the two circuits and optimizing their combined performance provides a single-stage driver. Because this approach allows the Circuit 3 and Circuit 4 functions to be bundled together, the overall driver size and parts count can often be reduced, making single-stage drivers ideal for lamps and other small SSL devices. Although it is difficult to produce PF values above 0.9 in small drivers using this approach, this level of performance is acceptable for low-power applications. Pictures of single-stage integrated drivers used in SSL lamps and small luminaires are shown in **Figure 1-4**.

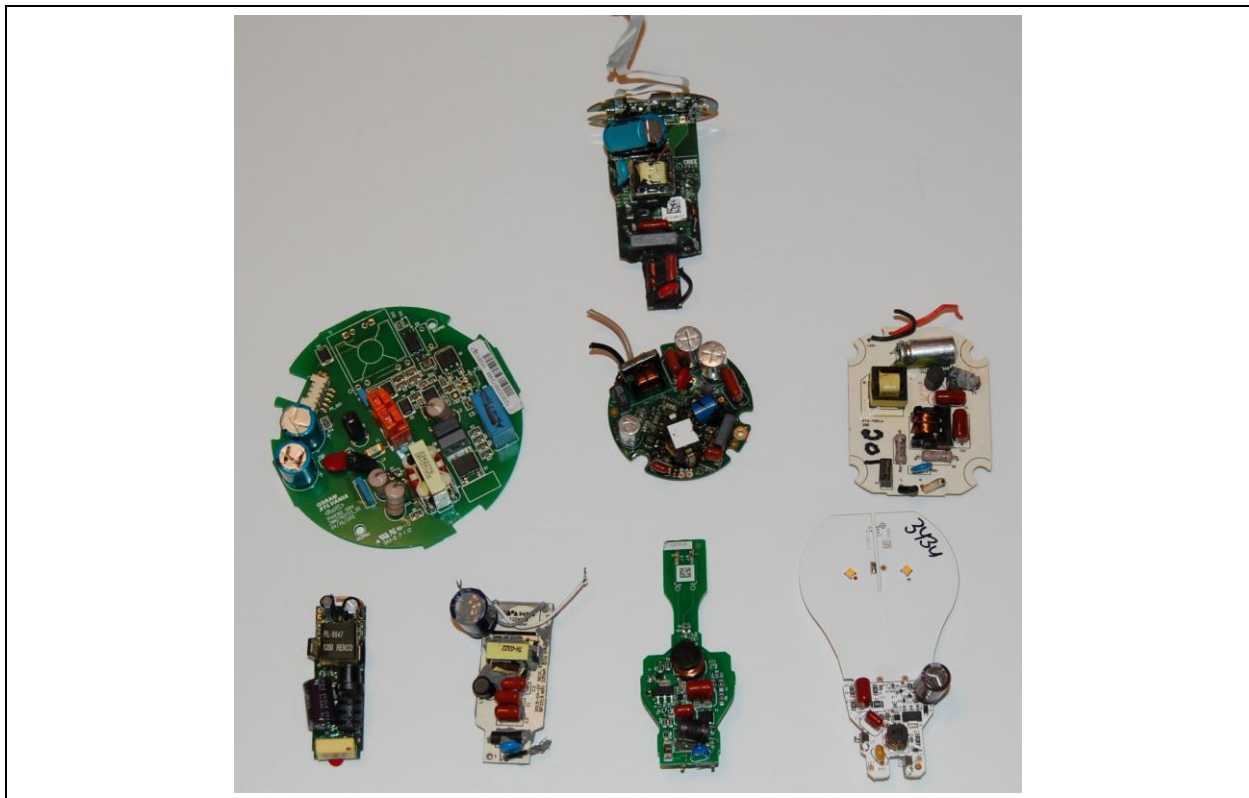


Figure 1-4. Pictures of single-stage drivers used in SSL downlights, PAR38 lamps, and A19 lamps.

If the performance of the PFC (i.e., Circuit 3) and dc–dc converter (i.e., Circuit 4) circuits are optimized separately, a two-stage driver with two power conversion stages is produced. In many two-stage designs, a flyback circuit is used in the PFC stage to produce an intermediate dc voltage with high PF and low THD, and a buck circuit is used for the final dc–dc conversion. This configuration is widely used in SSL drivers operating troffers, downlights, and other medium to large SSL fixtures. Pictures of typical two-stage drivers are shown in **Figure 1-5**.

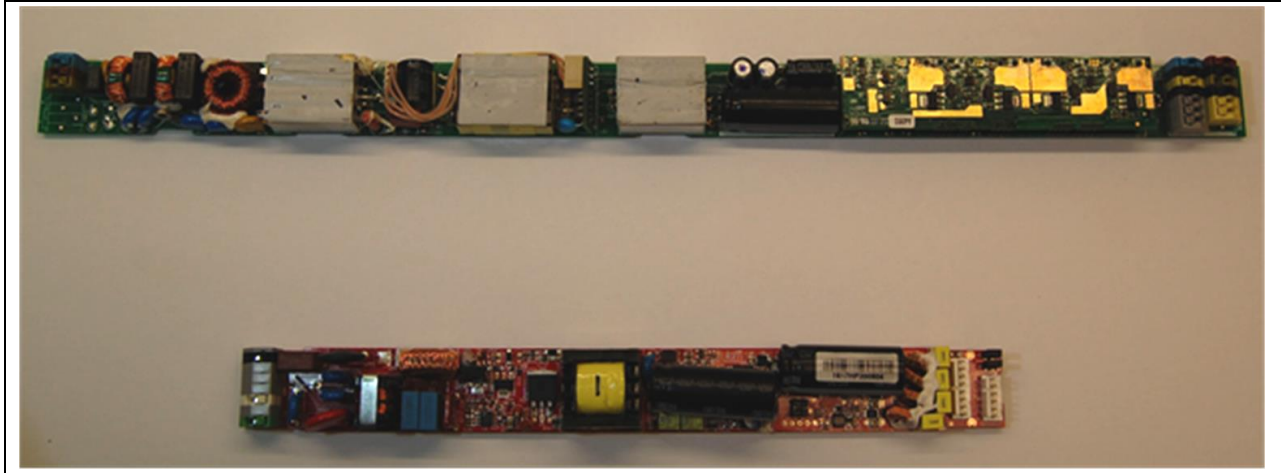


Figure 1-5. Two-stage drivers used in SSL troffers and downlights.

1.1.2 LED Properties

Drivers used in SSL devices are intended to produce illumination by providing electrical power to a light source composed of LEDs (i.e., the load). Often, these LEDs have similar emission characteristics and provide illumination of a fixed correlated color temperature (CCT). The Level 1 LED packages¹ that provide the light are surrounded by other SSL system components, including a printed circuit board (PCB) (i.e., the Level 2 package) that provides electrical connections between the LED packages and the driver, an optical system that shapes the LED emissions into the desired pattern, a thermal management system that handles waste heat in the LEDs and the driver, and an electrical driver that powers the LEDs [3].

Many SSL light sources have a fixed emission spectrum and can be operated with a single dc output from the driver. Such lighting sources utilize only one LED primary in the light source, and the LED primary is configured as a group of LEDs connected in series and/or parallel. All LEDs in this LED primary have similar emission characteristics (e.g., spectral power distribution and luminous flux), and each LED primary can be either a white emitter (e.g., warm white or cool white) or a color emitter (e.g., red, green, or blue) [4].

The ease with which multiple LED primaries can be incorporated into an SSL light source has opened the possibility of new lighting products with specially designed and dynamic emission properties. Light sources with high color rendering indices (CRIs) typically utilize a hybrid LED structure of two or more LED primaries in which a group of phosphor-converted LEDs (pcLEDs) are combined with one or more groups of direct-emitting LEDs (e.g., red or cyan) to produce white light. In these products, separate circuits provide dc power to the pcLEDs and direct-emitting LEDs, although the backend circuits are typically the same. Various commercial products with this architecture (e.g., A19 lamps, PAR38 lamps, and downlights) are available, and several have been studied by the U.S. Department of Energy (DOE) via the Commercially Available LED Product Evaluation and Reporting (CALiPER) program [5–8]. For most of these products, the distribution of electrical current between the two LED primaries was set at the factory, and the devices were not adjustable in the field.

Another example of combining multiple LED primaries into a single SSL source is TWL [4], which has many potential applications, including educational lighting [9–11], lighting in senior centers [12], and healthcare lighting [13]. A typical example is a linear TWL source comprising warm-white and cool-white LEDs. In this system, the two sets of LED primaries provide the end points of the tuning range. The combined emission

¹ Level 0 packaging refers to the LED die itself. Level 1 packaging refers to the packaged LED die. Level 2 packaging refers to packaged LEDs mounted on a PCB; this can also be termed an LED module.

spectra and corresponding CCT values can be adjusted in a linear fashion between the two end points by changing the current to each LED primary through separate driver channels [4, 10]. Because only linear tuning of the light is possible with two LED primaries, such tunable systems do not follow the blackbody locus; however, these systems provide the advantages of TWL with minimal system overhead. A more complex TWL system can be created using three or more groups of LED primaries. By varying the current provided to each LED primary, non-linear tuning of the white light emissions can be achieved, enabling the chromaticity of the source to follow the blackbody locus [4]. Several examples of LED modules composed of two or more LED primaries are shown in **Figure 1-6**.



Figure 1-6. Examples of LED modules comprising multiple LED assemblies for use in TWL devices.

Achieving the level of flexibility possible in tunable lighting systems and some high-CRI systems requires accurate control of the current going to each LED primary. This level of control can be attained using separate single-channel drivers for each LED primary; however, this approach introduces redundant electrical circuitry, which adds cost and weight to the finished product. An alternative approach is to use a single driver for all the

LED primaries but provide separate dc–dc conversion channels for each LED primary to control the power delivered to each. This driver configuration is termed a multichannel driver, and this device, together with its single-channel analog, are the focus of this report.

1.2 Driver Configurations and Common Use

Driver configurations vary with the LED lighting application to maximize device efficiency, minimize cost, and provide sufficient control to meet the specific LED lighting application. Some common driver configurations include the one-stage single-channel driver, two-stage single-channel driver, one-stage multichannel driver, and two-stage multichannel driver.

For SSL light sources with a fixed emission spectrum and only one LED primary, a simple, single-channel driver is commonly used because of the need for a single dc output for operation (in this case, a multichannel driver would only introduce unneeded circuitry). For many devices with limited space to house the driver (e.g., A-lamps and candelabras), a one-stage single-channel driver is used; some example circuits are presented in Figure 1-4. For devices that require more control over the dc supplied to the LED primary (e.g., dimming devices), a two-stage single-channel driver may be used. Although the two-stage driver offers better system control, it also increases the size and cost of the driver and often decreases the efficiency (because new circuit losses are introduced with the second stage).

For SSL devices that boast tunable-white capabilities, a driver is needed for each LED primary to capitalize on their properties because the individual power channels in a driver deliver specific dc waveforms to each LED primary. Such a driver can be constructed in one of two ways: 1) separate, single-channel drivers that are built for each LED primary or 2) one driver with multiple output channels (i.e., one output channel per LED primary). The latter approach is typically more economical because common electrical circuits (i.e., Circuits 1, 2, and 3; see Figure 1-1) can be shared between multiple channels.

Ideally, a one-stage multichannel driver would be used to operate a TWL system to minimize cost and space requirements. However, one-stage multichannel drivers require a very advanced control IC because the components in the LED driver's PFC stage are integrated with a dc–dc single-inductor multiple-output (SIMO) converter to provide a time-multiplexing control scheme to each LED primary. Although the SIMO converter has gained precedence in the literature, no devices in this study utilized a one-stage multichannel driver, likely because of the early development stage of the SIMO converter and the overall cost to develop the driver. Therefore, current TWL systems utilize either separate two-stage single-channel drivers for each LED primary or one two-stage multichannel driver to operate all LEDs.

Typically, two-stage multichannel drivers offer greater flexibility than multiple two-stage single-channel drivers because the control systems for multichannel drivers tend to be more advanced. For example, in a typical two-stage, single-channel system, the user can select well-defined, preset CCT and dimming values at a low cost, but is not offered the flexibility to deviate from the preset values because the control ICs between each single-channel driver are minimally integrated [14]. In contrast, greater integration and communication between LED primaries in a multichannel driver system affords a user the added capability to override intensity and CCT values and to program the driver to change intensity and color temperature with natural sunlight (daylight harvesting). These features, along with lower cost (in many cases) compared to multiple drivers, make two-stage multichannel drivers attractive for consumers who want greater control over the CCT value (e.g. marketing businesses) and/or wish to optimize energy savings (e.g. businesses with ample natural sunlight). A detailed look into two-stage drivers is provided in the remainder of this report.

1.2.1 Basics of Driver Structure

In a two-stage, single-channel driver for LED devices, Stage 1 primarily functions to convert ac power to intermediate dc power with appropriate PFC and THD properties (i.e., Circuits 1, 2, and 3); often, a boost or flyback driver topology operated under the control of an IC is used for this conversion. The intermediate dc voltage produced by Stage 1 is then fed to the dc–dc conversion circuit, which is operated by a second control

IC, to provide the power for the LED primary. The two stages communicate with each other through their control ICs (**Figure 1-7**). Figure 1-7 presents a generalized schematic of a two-stage single-channel driver; additional components (e.g., capacitors, inductors, resistors, and MOSFETs) associated with different driver typologies are omitted for convenience.

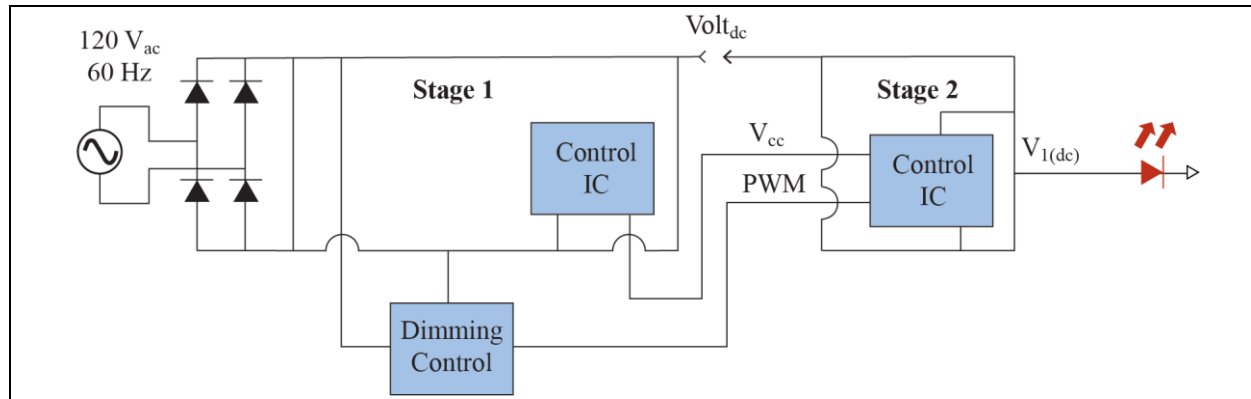


Figure 1-7. Schematic of a two-stage single-channel driver.

Often, these devices contain additional circuitry to add a user interface panel for control inputs where the light intensity and, in the case of two or more single-channel drivers operating together to power two or more LED primaries, CCT can be modified (**Figure 1-8**). These single-channel systems offer good efficiency and control of the LED primaries, but again, they suffer from redundant circuitry.

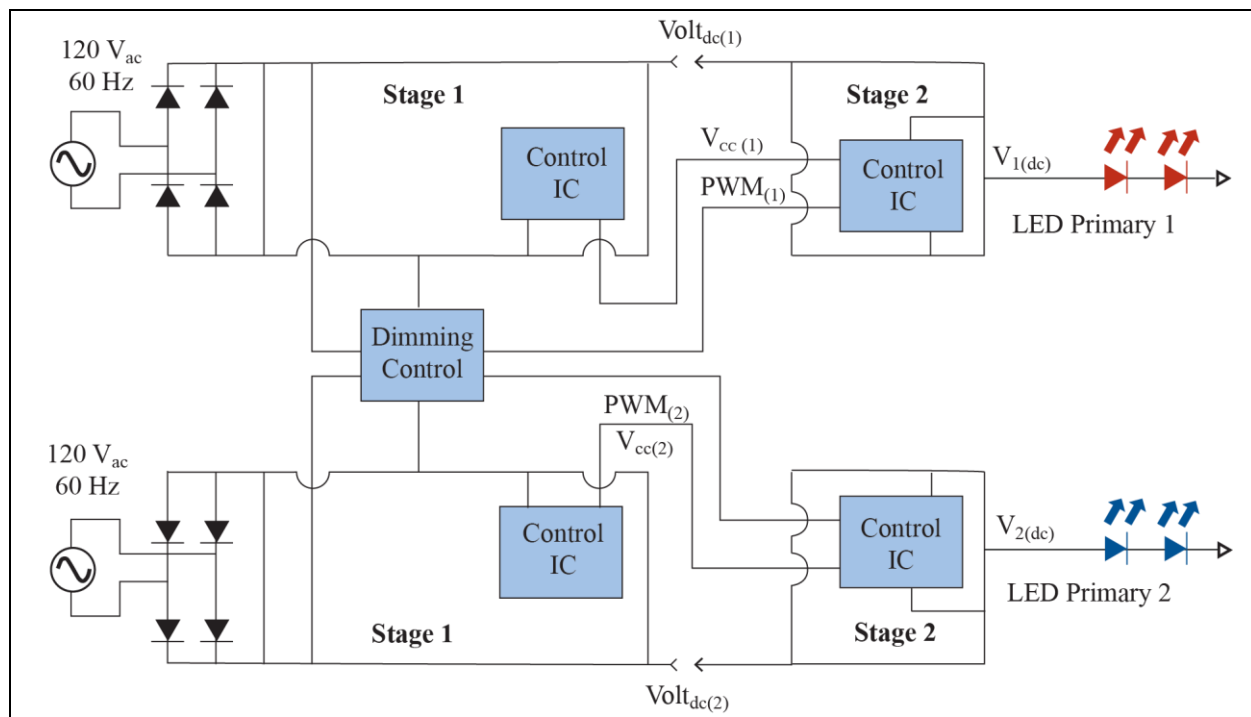


Figure 1-8. Schematic of multiple two-stage single-channel drivers combined with a user interface (e.g., dimming control) in a TWL system with two LED primaries.

1.2.2 Two-Stage Multichannel Drivers

A two-stage multichannel driver for LED devices operates in a manner comparable to that of a two-stage single-channel driver. Again, Stage 1 primarily functions to convert ac power to high-voltage dc power (i.e.,

Circuits 1, 2, and 3). However, the setup of Stage 2 is different: the LED primary channels in Stage 2 share the intermediate dc power supplied by Stage 1 (i.e., the LED primary channels share the ac-to-dc power conversion circuits). This architecture is advantageous because it reduces the number of components necessary on the PCB, thereby reducing cost and driver size. The two stages communicate with each other through their respective control ICs (**Figure 1-9**). Again, Figure 1-9 presents a generalized schematic of a two-stage dual-channel driver; additional components (e.g., capacitors, inductors, resistors, and MOSFETs) associated with potential driver typologies are omitted for convenience.

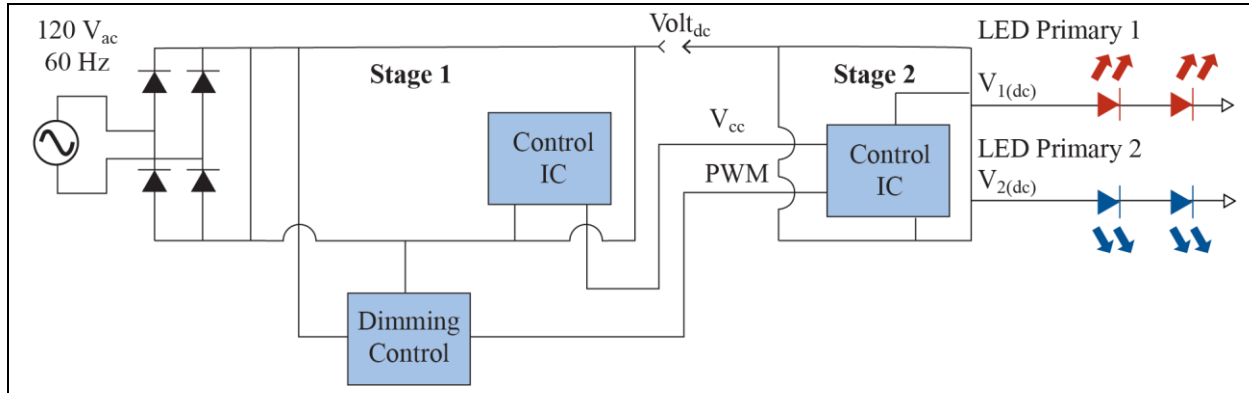


Figure 1-9. Schematic representation of a two-stage dual-channel driver for operating a TWL system with two LED primaries.

The controllability of the two-stage driver is built primarily into the second stage. As such, a detailed view of the second stage in the two-stage multichannel driver is provided. Typically, the driver configuration of Stage 2 is a buck topology, which is a relatively simple dc controller consisting of a MOSFET, an inductor, a capacitor, and a diode configured as shown in **Figure 1-10**.

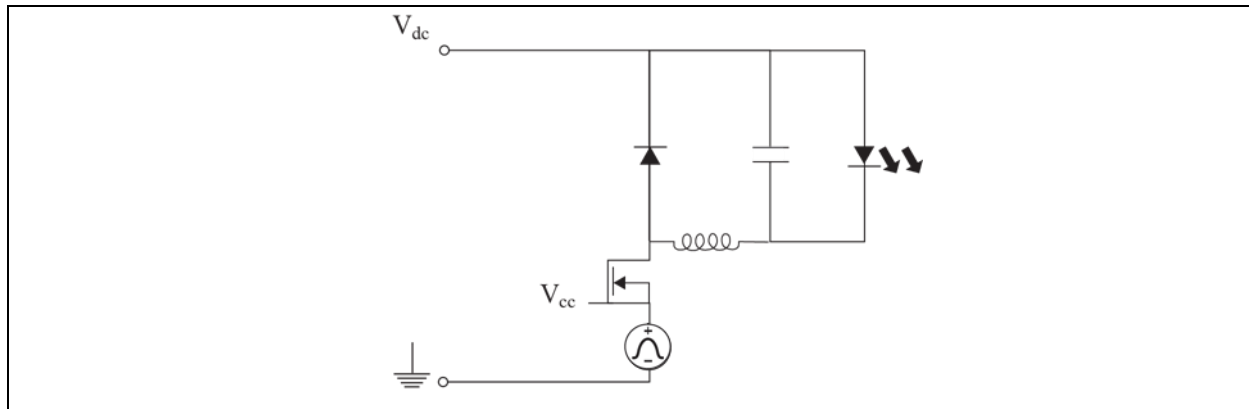


Figure 1-10. Detailed schematic of the buck converter often used to control the dc output to the LEDs in a two-stage multichannel driver.

To control each LED primary, inputs from both the user (through the user interface) and the control IC of Stage 1 are needed. The user input (e.g., a change in the desired CCT or dimming level) is relayed to the control IC of Stage 2 through a pulse width modulation (PWM) signal. When the signal enters the control IC of Stage 2, a series of logic gates and other components individually adjusts the duty cycles of the MOSFETs in the different buck channels. Recall that a duty cycle close to 1 applies a small reduction to the average power delivered to the LED (from the dc power supplied by Stage 1), and a duty cycle close to 0 applies a large reduction to the average power delivered to the LED. Through these adjustments, the necessary power is supplied to each LED primary circuit to obtain the light output from each needed to fulfill the new

circumstances (**Figure 1-11**). The buck circuits providing the output voltages to each LED primaries are included in Figure 1-11 for convenience.

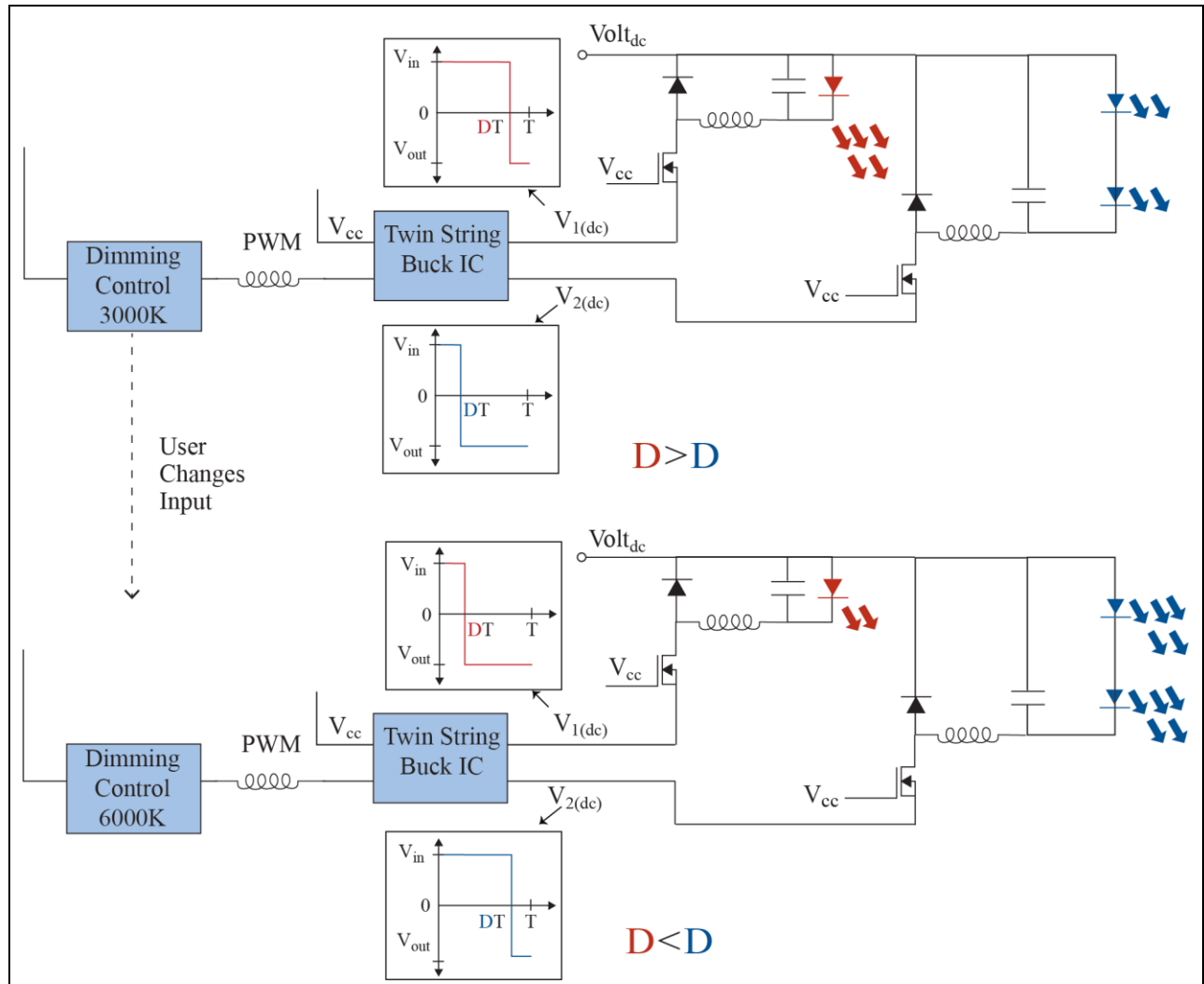


Figure 1-11. Schematic illustration of the operations of a TWL with two LED primaries.

2 Test Samples

The devices under test (DUTs) discussed in this report were subjected to aging through either room temperature operational lifetime (RTOL) testing or accelerated stress testing (AST) to minimize the test time. All DUTs tested were two-stage drivers, and the samples included a mix of single-channel drivers (three products) and multichannel drivers (three products). Each driver was intended for use in troffers, street lights, and other relatively large luminaires. All drivers tested were separate devices that are often bolted to luminaire frames and connected to LED primaries through external wiring. A list of the samples examined in this report is provided in **Appendix A**. The drivers were assigned numbers based on whether they were single output channel products (DUT-S1, DUT-S2, and DUT-S3) or multiple output channel products (DUT-M1, DUT-M2, and DUT-M3). Two samples of each driver were tested in this study, and a third sample of each was maintained as a control.

Several earlier DOE reports included test data on hybrid LED devices requiring multiple outputs to the different LED primaries. In addition to providing insight into the operation of integrated, multiple output channel drivers, these previously published data can facilitate comparisons with the current study and are included here for convenience. In general, these devices with hybrid LED light sources (and multichannel drivers) performed well in CALiPER testing conducted for the DOE by the Pacific Northwest National Laboratory. The hybrid LED A19 and PAR38 products used in CALiPER 3 [5] and CALiPER 20 [6, 7] testing are also listed in Appendix A for convenience, although a detailed analysis of the data obtained from these products is not included in this report.

A 6" downlight containing a hybrid LED source and an integrated multichannel driver was also addressed in a previous DOE report on highly accelerated stress testing (HAST) of luminaires (known as the Hammer Test) [8]. A more detailed analysis of this product is included in the present report because the structure of the driver used in this product is analogous to that used in multichannel drivers for TWL. Two samples of this product were subjected to RTOL testing for more than 3 years, and the results are presented here and compared to the Hammer Test results.

All the DUTs discussed in this report had separate buck converter stages for each channel, as shown in Figure 1-11. Thus, there is a single control IC for all channels but separate MOSFETs, buck inductors, and capacitors for each channel. For most DUTs in this study, the MOSFETs, inductors, and capacitors were discrete components placed on the PCB. However, for DUT-M3, the MOSFETs are integrated into the control IC (the inductors and capacitors remained as discrete components on the PCB) [15]. Although this higher level of integration does reduce board space, it also places increase demand on the thermal management of the combined package because the heat dissipation requirements of MOSFETs and control ICs often differ. A similar effect has been observed in other devices where a MOSFET and control IC are combined in the same package [16].

3 Experimental Procedures

3.1 Accelerated Stress Tests

The stand-alone drivers examined in this study were subjected to AST at nominal conditions of 75°C and 75% relative humidity (7575). These conditions were chosen because previous studies demonstrated that the 7575 environment provided reasonable acceleration for integrated SSL drivers used in 6" downlights [16]. In that previous study, 38% of the population of 6" downlights (28 out of 74) exhibited electrical failure in less than 2,500 hours of exposure to 7575.

During AST exposure, the DUTs were placed inside a temperature and humidity chamber, as shown in **Figure 3-1**. The LED loads were placed external to the chamber but were connected to the drivers through wires that passed through openings in the chamber walls. Once both the power and load connections were made, the openings were sealed to reduce the escape of heat and humidity from the chamber, as shown in **Figure 3-2**. An opening on top of the chamber was not closed and allowed for the controlled loss of heat and humidity. The chamber compensated for this loss and maintained the temperature within $\pm 2^\circ\text{C}$ and the relative humidity within $\pm 5\%$. This testing setup allowed the drivers to be exposed to the 7575 environment while maintaining the LED primaries in a room temperature environment. Consequently, only the drivers were stressed by the AST conditions, isolating any effects attributable to the aging of the driver caused by the load.



Figure 3-1. Configuration of the DUTs during AST exposure and the connecting wires to the ac source and the LED loads.

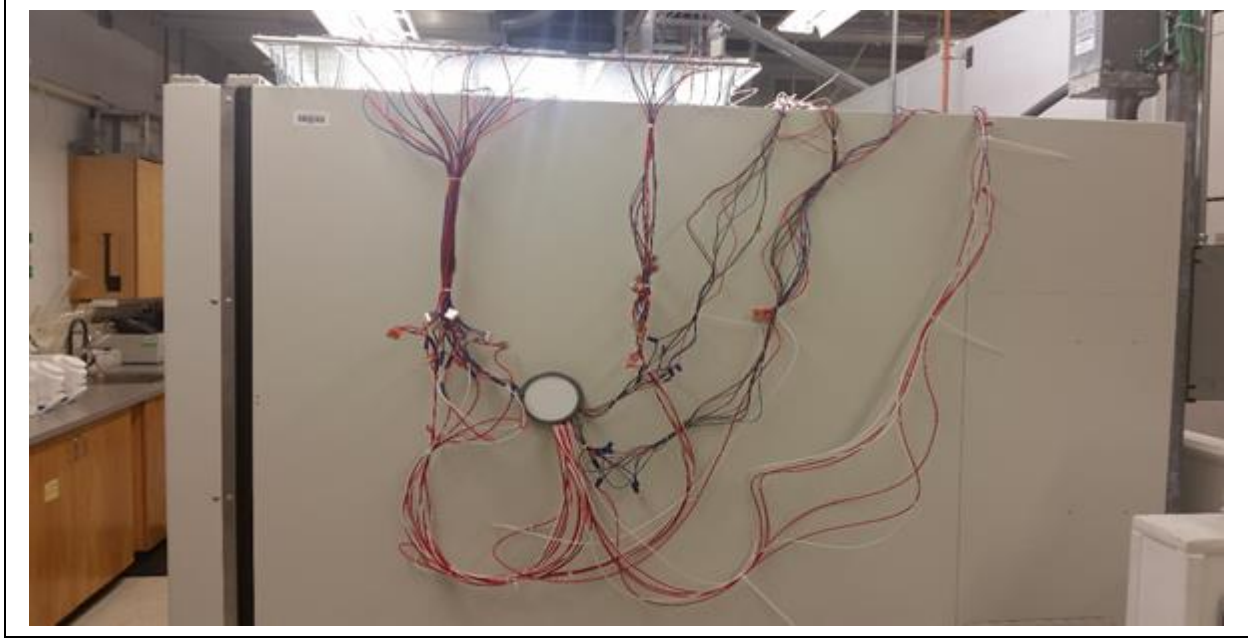


Figure 3–2. Exterior of the test chamber showing the LED loads on top of the chamber and the connecting wires to the DUTs.

3.2 RTOL Testing

Two samples of the Cree LR6 downlight, with integrated multichannel driver, were mounted in the ceiling of an office at RTI International, as described in the Hammer Test report [8]. The samples were operated continuously in a typical office environment for more than 3 years, except for when they were removed from the ceiling for testing, which occurred roughly every 6 months. Photometric measurements were taken in a large integrating sphere. Then, the devices were returned to the ceiling for continued testing. The Cree LR6 downlights tested in this manner were not subjected to any AST protocols during their test periods, although other samples of this product were subjected to the Hammer Test, as reported previously [8].

3.3 Accelerated Testing Methods

During the tests reported here, the stand-alone drivers were subjected to AST conditions of 7575 for a total of 2,500 hours. Future reports will describe subsequent testing of the samples that survived this level of exposure. During the current tests, power to most DUTs was provided on a one-hour duty cycle (i.e., one hour on and one hour off). The lone exception was DUT-M1, which was on a two-hour duty cycle because of its larger mass. Environmental exposure of the DUTs was typically performed in increments of 500 hours until the cumulative exposure reached 2,500 hours, and the degradation of the DUTs was monitored during the tests and at the end of each 500-hour time increment. Various test methods were used during and after the 7575 exposure, including measurement of the temperature rise of the DUTs during power cycling, electrical characterization of the drivers, and photometric measurements, including flicker. Measurements were generally taken at room temperature, although a few select photometric measurements were taken under 7575 conditions, as discussed below.

3.4 Measurement Methods

3.4.1 Temperature

As an initial experimental step, the temperature rise of key components was measured for the single-channel drivers using chromel alumel thermocouples (TCs). The top of each driver was removed, and TCs were placed directly on select components, including the PCB, electrolytic capacitors, inductors, transformers, MOSFETs, and control ICs. The components with the greatest temperature rise tended to be the flyback transformer and

the power MOSFET on each driver. The temperatures of these components were typically 25°C to 30°C above ambient. After replacing the top of the driver, the temperatures at locations on the top and bottom of the case near these components were also measured. These measurements helped to identify hot spots in the driver that could be tracked by applying external TCs to the top and bottom of each DUT during AST exposure.

In general, the TCs were attached at the location on the case nearest to the flyback transformer in the PFC circuit and the switching MOSFET in the dc–dc converter. The TC readings enable observing the temperature swing in the device during power cycling in the AST environment. An example of the temperature swing on a component inside a driver during 7575 is given in **Figure 3-3**.

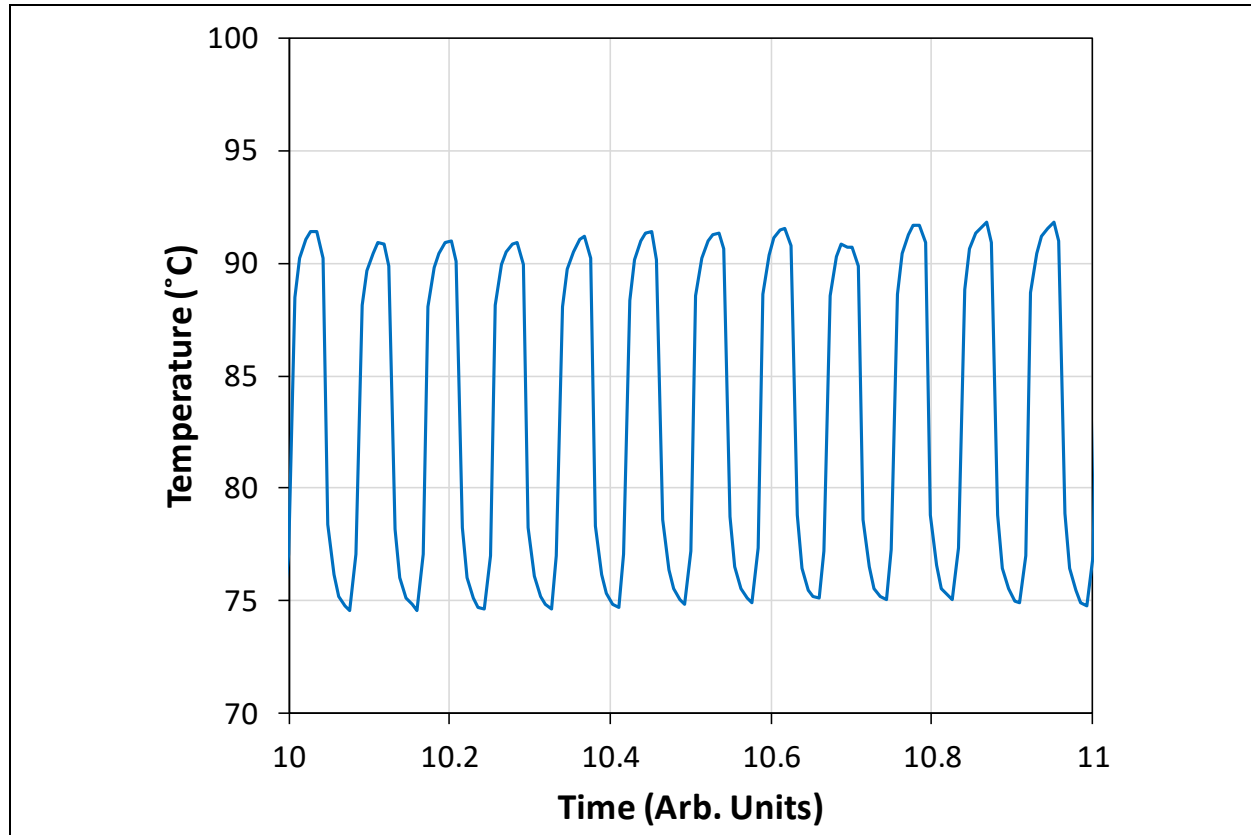


Figure 3–3. Temperature measurement of an integrated IC and MOSFET package on a multichannel driver undergoing AST.

3.4.2 Electrical

The power characteristics of the multichannel drivers (DUT-M2 and DUT-M3) examined in this study were tested after 2,500 cumulative hours of 7575 exposure using a Xitron 2802 two-channel power analyzer and compared to an unexposed control driver of the same product. The driver and LED loads were configured as for the 7575 experiments except that external connections were made to the power analyzer to measure (1) the input ac mains power and (2) the output dc power supplied by the driver to each channel. To make the power measurements, channel 1 of the Xitron 2802 power analyzer was configured as an output channel, while channel 2 was configured as an input channel:

- **Channel 1:** dc power supplied by the driver was connected to channel 1 of the power analyzer before being fed into one of the LED load output channels (any remaining LED load output channels stayed directly connected to the LED driver). Once an LED load output channel was characterized, the next LED load output channel was connected to channel 1 of the Xitron 2802 power analyzer, and the process was repeated.

- **Channel 2:** ac mains power was connected to channel 2 of the power analyzer and then fed to the power connections of the test driver.

Each driver channel was tested at 100, 75, 50, 25, and 1 percent dimming for the DUT-M2 and DUT-M3 samples using a digital multiplex (DMX) dimming controller. dc measurements were recorded for each channel of the driver, allowing the overall driver efficiency to be calculated. The peak inrush current was set to 90°. Peak current inrush data, THD, ripple, and other ac and dc voltages and currents were recorded using a computer and the Xitron application.

The single-channel drivers (i.e., DUT-S1, DUT-S2, and DUT-S3) examined in this study were tested before and after 2,500 hours of 7575 exposure by Hubbell Lighting Inc. using a Chroma LED power driver test system. In this test, the input voltage was varied to examine any changes in driver performance. Among the output parameters measured were device efficiency, output power, and PF. Additionally, the driver's dimming characteristics were measured with a 0–10-V dimming circuit initially and after 2,500 hours of exposure.

3.4.3 Photometric

Because the LED loads were placed on top of the test chambers, the photometric properties could be readily measured at any time during AST exposure. Although this configuration was expected to ensure that the emission characteristics of the LEDs remained constant during the test, degradation in the driver circuitry could negatively impact LED emission and produce increased flicker and reduced emissions. To monitor any degradation of the LED output, a handheld spectral flicker meter (GigaHertz-Optik BTS256-EF), operating under computer control, was used in conjunction with an integrating sphere. This configuration allowed a number of photometric properties to be measured for each sample with minimal interference from the other samples and the overhead lights. A list of the photometric properties recorded during this study is provided in **Table 3-1**.

Table 3-1. Photometric properties measured during this study with the GigaHertz-Optik BTS-256-EF.^a

Photometric Property
Illuminance waveform with time
Total illuminance
Maximum illuminance
Minimum illuminance
Frequency resolution ^b
Flicker % ^b
Flicker index ^b
Spectral power distribution
Chromaticity coordinates
CCT

^a See reference [17] for an overview of flicker meters.

^b Frequency resolution was 12.5 Hz

4 Findings

4.1 Cree LR6 Downlight

The Cree LR6 is a first-generation LED downlight product that was first examined by RTI during the Hammer Test [8]; a modified version of this product is described elsewhere [18]. The driver for the Cree LR6 contains two power conversion stages that are integrated into the housing and heat sink, a flyback converter for Stage 1, followed by a buck converter consisting of three separate, controllable output channels. The light engine attached to this driver contains three different LED primaries, and in one version of this product, the three LED primaries are a green-yellow pcLED, a cyan direct-emitting LED, and a red direct-emitting LED, as shown in **Figure 4-1**. The buck inductors for the three LED primary channels are also labeled in Figure 4-1. Although this product cannot be manually tuned, a photosensor detects the properties of the light produced by the device and automatically adjusts the power supplied to the three LED primaries to maintain the luminous flux level and chromaticity point. This capability does provide a means varying the chromaticity, although it is not under external control.

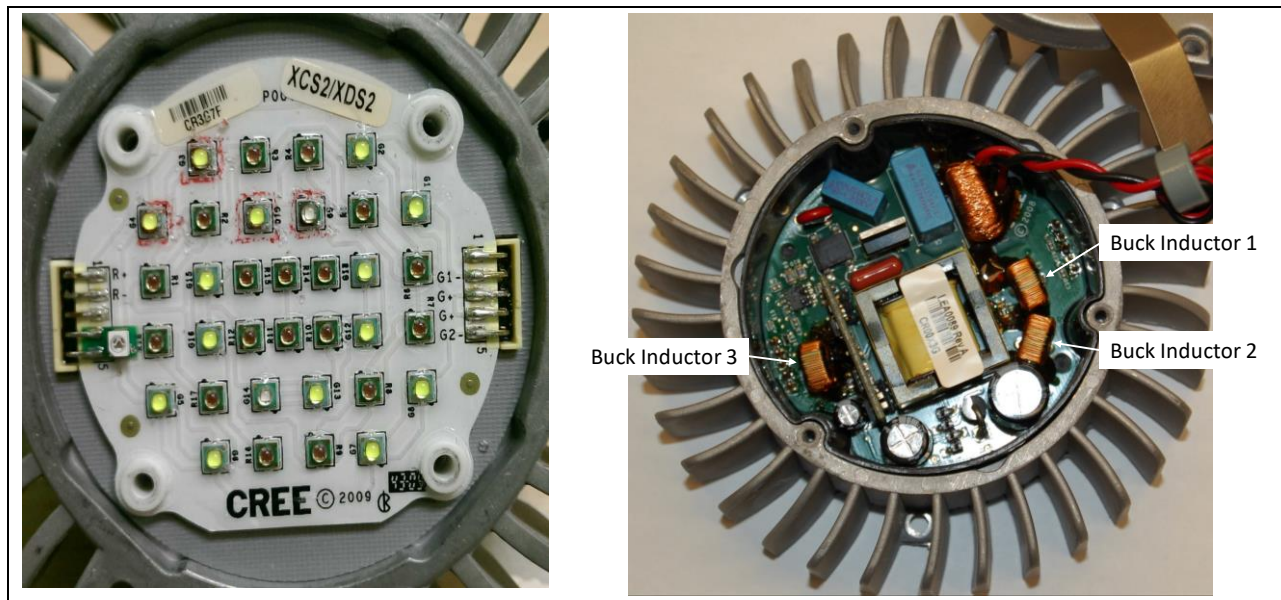


Figure 4-1. LED light source and driver for the Cree LR6 downlight.

One of the first publicly available studies that addressed the robustness of LED luminaires was the Hammer Test conducted by RTI in association with the LED Systems Reliability Consortium and the Next Generation Lighting Industry Alliance [8]. The Hammer Test is a HAST protocol that consists of four sequential HAST environments:

- Steady-state temperature and humidity testing at 85°C and 85% (8585) relative humidity for 6 hours;
- Temperature shock for 15 hours between -50°C and 125°C with a 30-minute dwell time at each extreme;
- A second round of steady-state temperature and humidity testing at 8585 for 6 hours; and
- High-temperature operational life testing at 120°C for 15 hours.

One loop of the Hammer Test requires 42 hours to complete, and the DUTs are continually cycled through the test until failure occurs. The samples were removed from testing for photometric measurements after every five loops of the test and then reinserted into the test. The primary goal of the Hammer Test was to stress LED

luminaires in a manner that would create failures so that these failures could be analyzed further to understand the robustness of the LED devices. The Hammer Test is not intended to be a standardized test for measuring LED devices [8].

In the Hammer Test report, the Cree LR6 luminaire samples were labeled as Luminaire A. Board-level failures were observed for each sample of this product, likely because of the extreme temperature shock conditions, which may not reflect the conditions experienced during normal use [8]. In general, in the Hammer Test, the Cree LR6 samples exhibited excellent lumen maintenance, as shown in **Figure 4-2**, until the onset of device failure. During testing, all three samples eventually exhibited excessive photometric flicker near their end of life and were ultimately considered parametric failures because of low luminous flux and high flicker. The appearance of flicker in these samples can be traced to the board issues caused by the temperature shock portion of the test and were not a direct result of LED degradation. When the LR6 samples began to fail, the luminous flux dropped sharply, as shown for Sample 3 in Figure 4-2, as the control system adjusted the output to maintain the color point. However, as shown in **Figure 4-3**, the chromaticity point continued to drift in the yellow direction (i.e., both u' and v' increased with time).

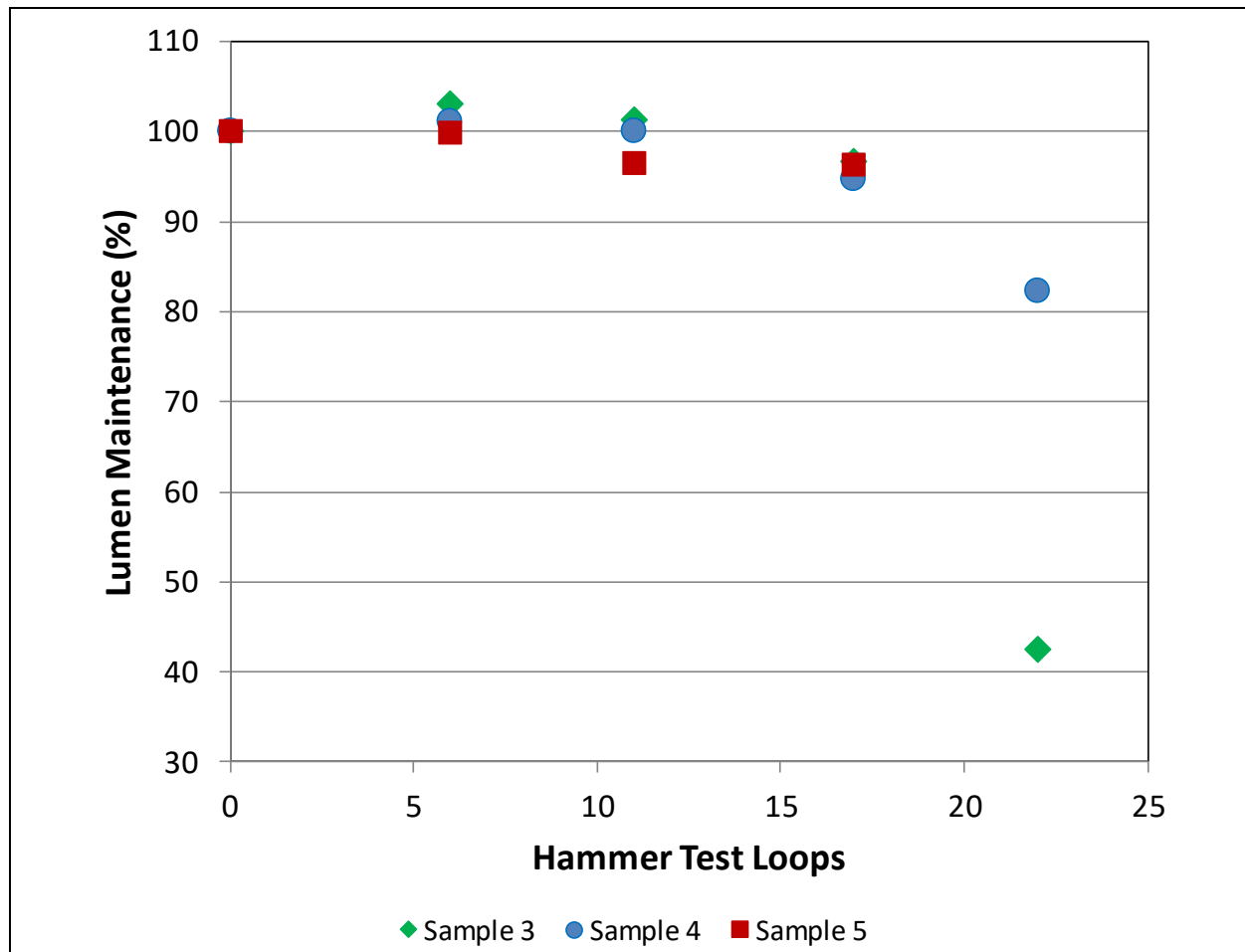


Figure 4-2. Luminous flux maintenance of three Cree LR6 luminaires subjected to the Hammer test [8].

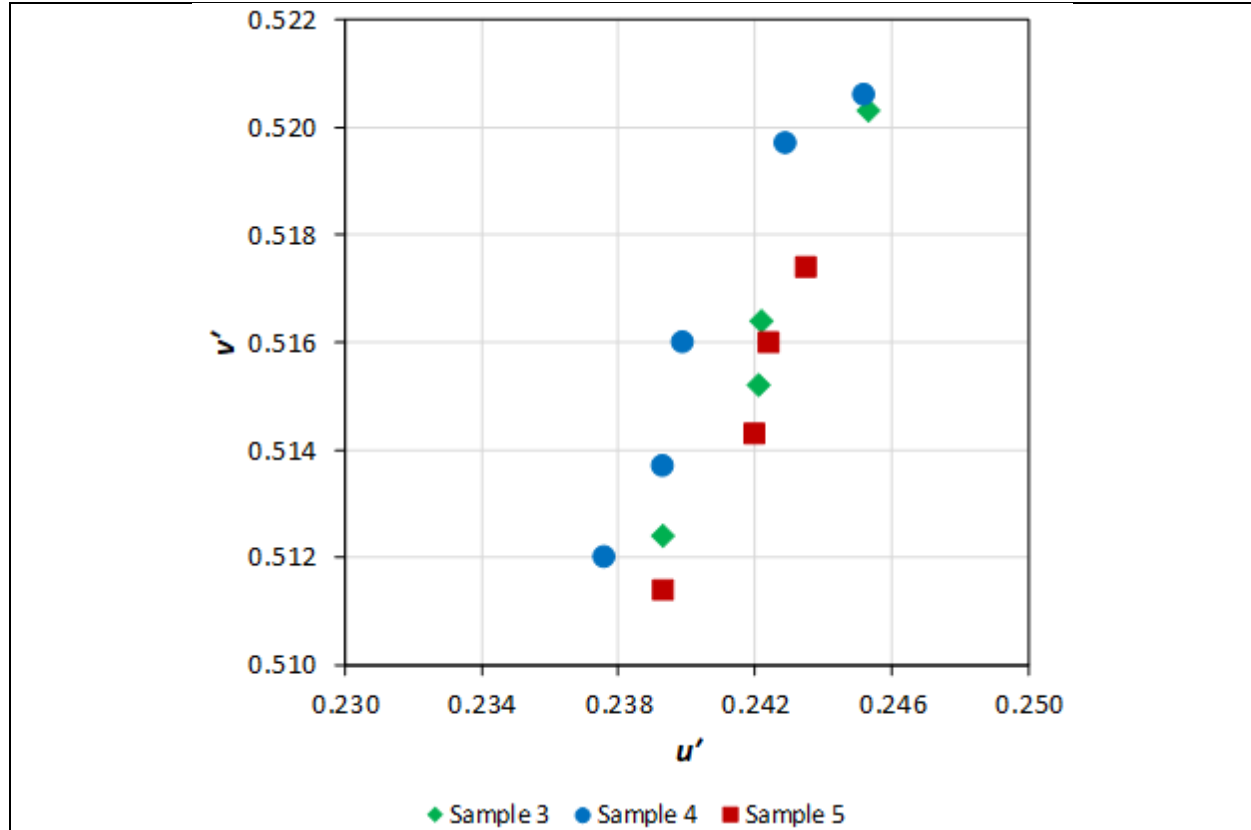


Figure 4-3. Change in the chromaticity coordinates of Cree LR6 luminaires during the Hammer Test.

As part of the control for the Hammer Test, two samples of the Cree LR6 product were continuously operated at room temperature for more than 3 years. In this RTOL test, the test samples maintained luminous flux levels exceeding 90% for more than 3 years (NOTE: 3 years is 26,298 hours), as shown in **Figure 4-4**. However, although the luminous flux levels remained high, the chromaticity shifted initially in the generally blue direction (i.e., both u' and v' decreased with the change in v' being larger) and then in the generally yellow direction (i.e., v' increased and u' changes little), as shown in **Figure 4-5**. This chromaticity shift behavior and the drop in luminous flux agree with the phenomena observed during the Hammer Test, as discussed above, illustrating the potential utility of HAST testing (e.g., the Hammer Test) for elucidating potential failure mechanisms. The chromaticity shift behavior is a Chromaticity Shift Mode (CSM)-3 chromaticity shift, which is often observed in high-brightness pcLED sources [7]. Eventually, the aging of the LEDs exceeded the ability of the driver to adjust the current levels to the LED primaries, and the device reduced the luminous flux to maintain its chromaticity, as shown in Figure 4-4. As this degradation process continued, the luminous flux dropped, and the chromaticity began to deviate sharply from the behavior found during the first 3 years of operation, as shown for Sample 2 in Figure 4-5.

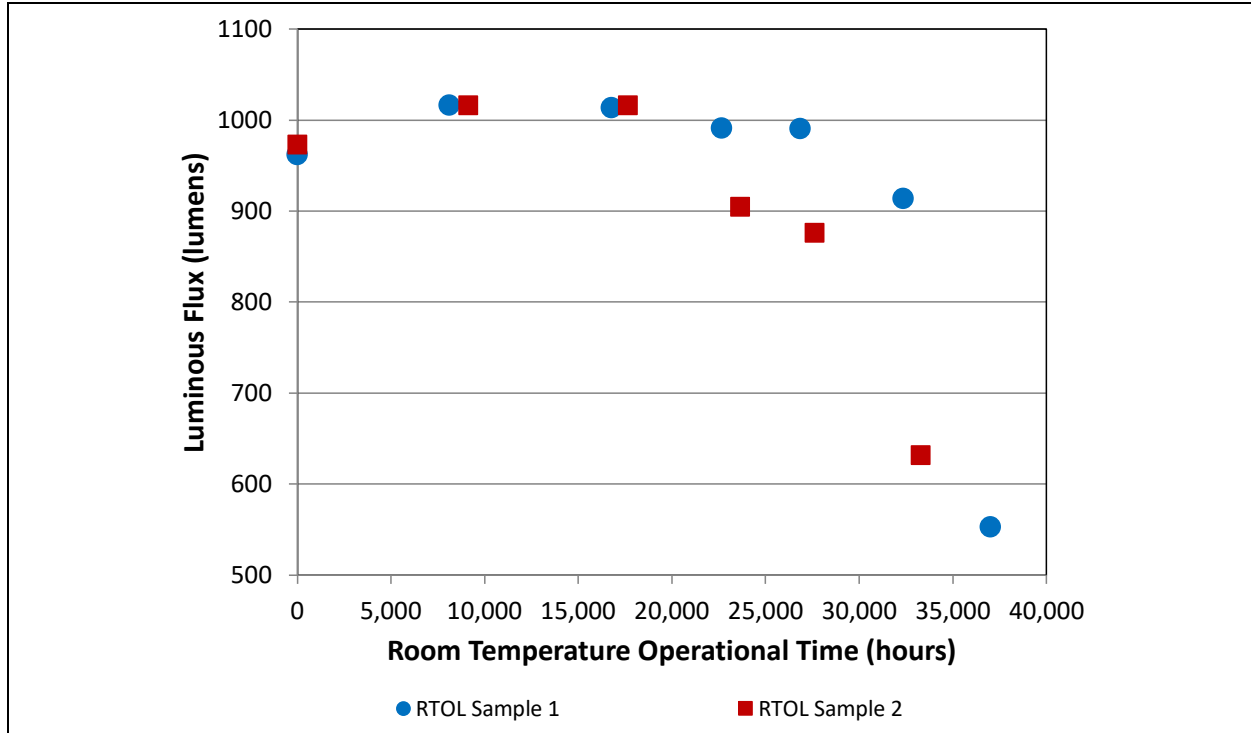


Figure 4-4. Luminous flux maintenance of the Cree LR6 samples during RTOL testing.

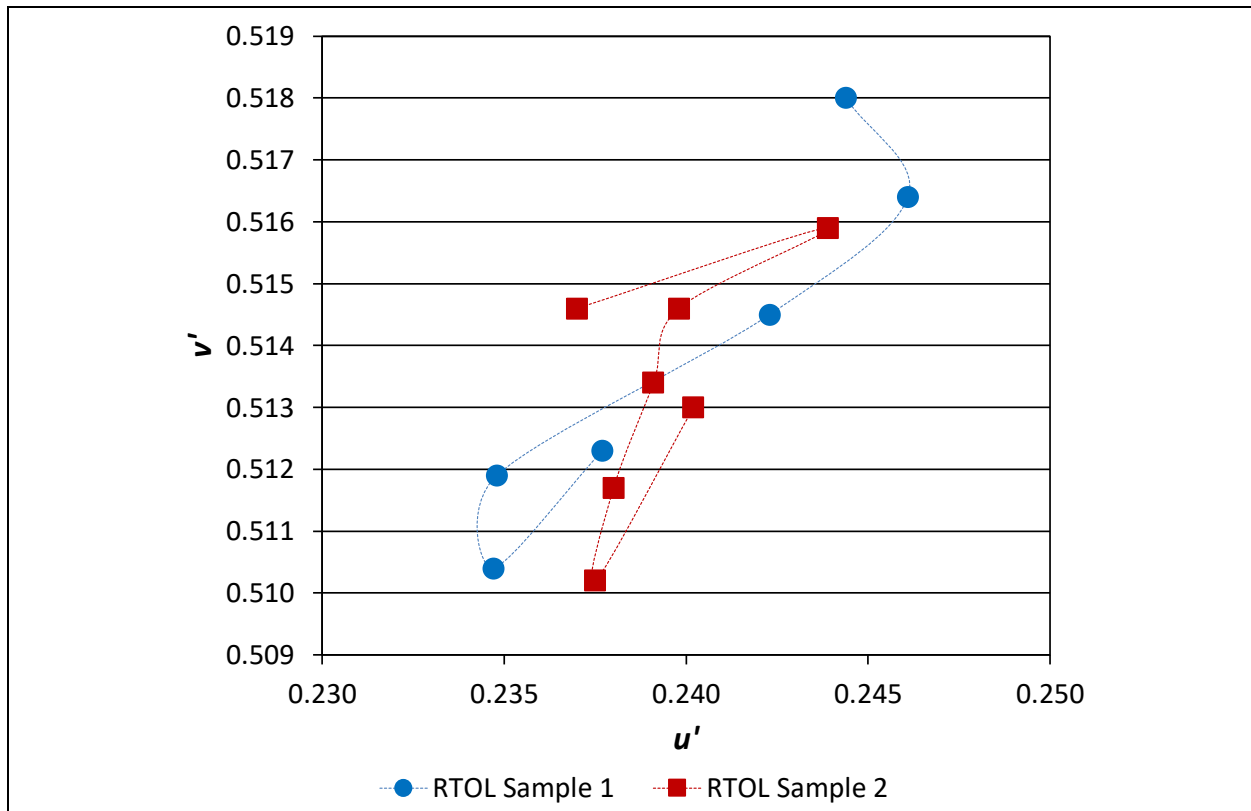


Figure 4-5. Chromaticity shift of the Cree LR6 samples during RTOL testing.

As the RTOL testing of the LR6 luminaires continued, photometric flicker became a significant issue that ultimately resulted in the removal of both devices from testing as parametric failures. Sample 1 failed parametrically after approximately 3.8 years of continuous use, and Sample 2 failed after roughly 4.3 years. In both cases, the onset of excess photometric flicker was abrupt, although the luminous flux of both dropped sharply, as revealed by integrating sphere measurements taken before the flicker was visually apparent. This decrease is indicative of a pending failure, but the level of flicker was not sufficient to remove the sample from testing. Subsequently, after the fixture was reinstalled in the ceiling, the level of photometric flicker became great enough to require the device to be removed from testing.

The photometric flicker of each failed LR6 was tested as described in Section 3.2.3. For comparison purposes, the photometric flicker waveform of a control LR6 was also examined, and the flicker profile of this device is shown in **Figure 4-6**. The measured photometric flicker of Sample 1 after parametric failure is given in **Figure 4-7**, and a comparison of the photometric flicker metrics of the control and failed devices is presented in **Table 4-1**. A failure analysis of both devices traced the root cause of the parametric failure to solder joint failures on some LEDs in the LED module and not to driver-related issues. This conclusion was based on the finding that some, but not all, of the LEDs within a given LED primary were not functioning during the flicker state. Probing the LED board caused some of the non-functioning LEDs to begin operating; however, a deeper evaluation was not possible because the LED board was covered with a conformal coating. When proper operation of the LEDs was achieved after probing the board, the flickering ceased. Thus, the loss of LEDs caused by solder failure may have changed the LED load, resulting in an unstable state for the driver, and the observed flicker was a consequence of this unstable operation. This example demonstrates that when examining the performance of a driver, it is also important to consider any changes in the load and their impact on driver performance.

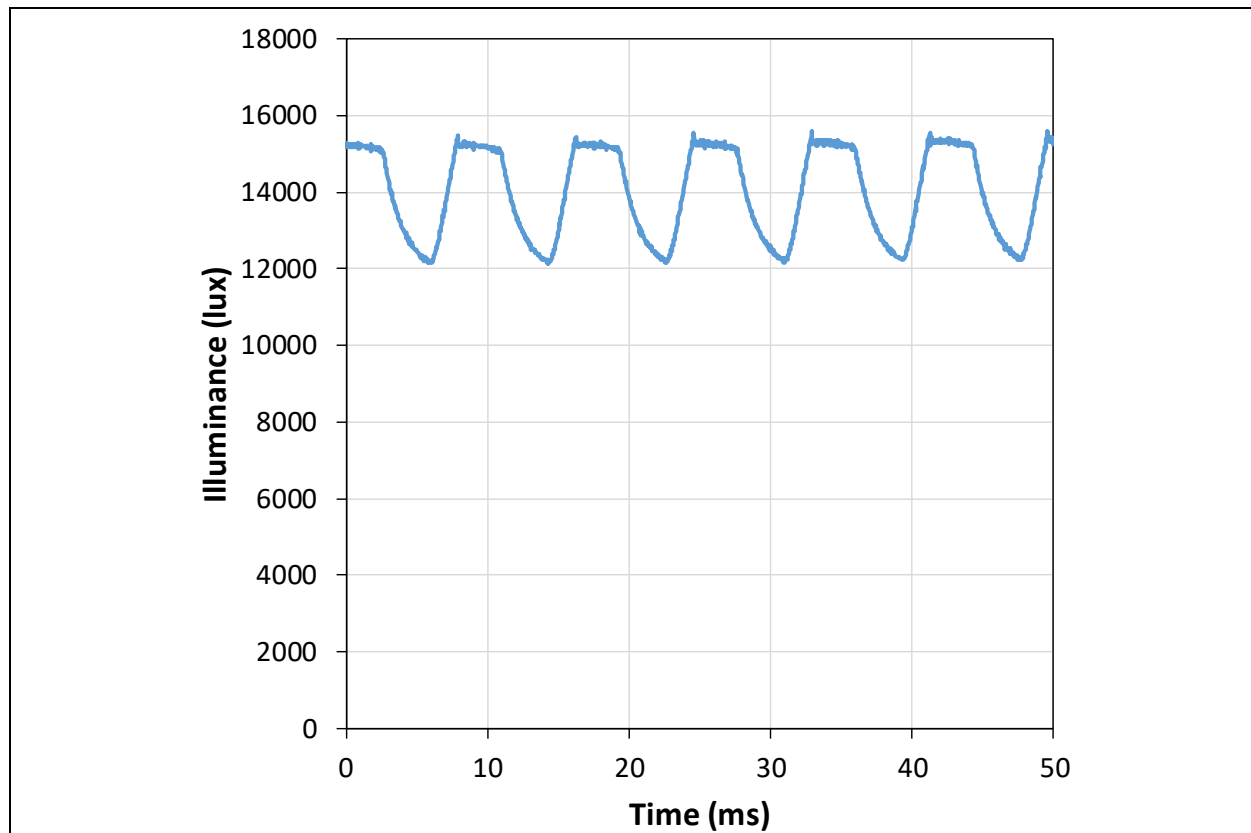


Figure 4-6. Flicker profile of the control Cree LR6.

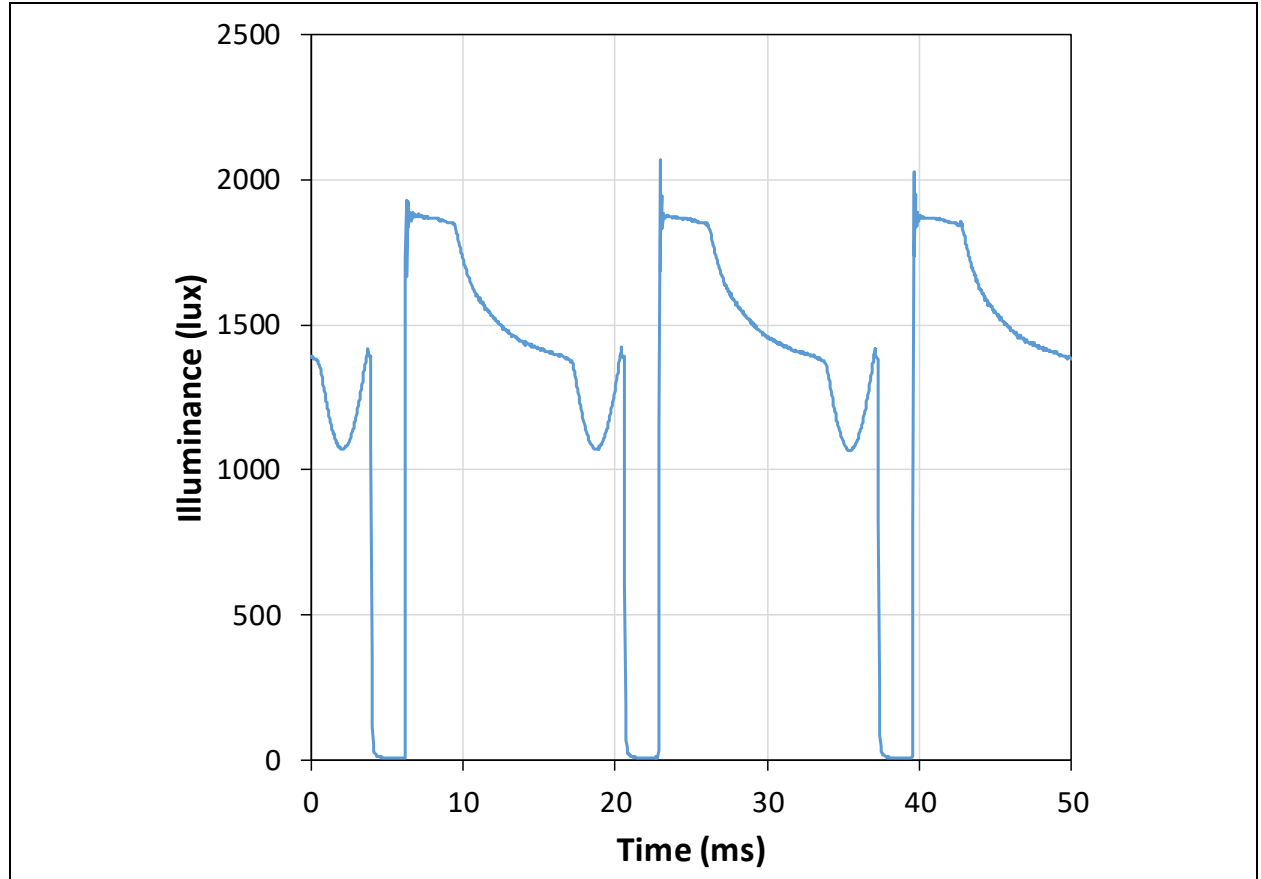


Figure 4-7. Photometric flicker waveform of an LR6 device (Sample 1) that failed during RTOL testing.

Table 4-1. Comparison of the photometric flicker parameters of the failed RTOL and control LR6 samples.

Property	Control	Sample 1
% Flicker	12.7%	99.6%
Flicker Index	0.0391	0.1532
Flicker Frequency	120 Hz	60 Hz

4.2 Single-Channel Drivers

Three different single-channel driver products were exposed to the 7575 environment, each for a total of 2,500 hours. Two samples of each product were examined during this test. All three products were Class 2 drivers that can operate at input ac voltages between 120 V and 277 V, although all devices were operated at 120 V during these tests. In addition, all three products were rated for surge protection of 2.5 kV (per IEEE C62.41), equipped with 0–10 V dimming controls, and qualified for the Underwriter’s Laboratory damp and dry environmental protection rating. The interiors of DUT-S1 and DUT-S3 were encapsulated with a hard, black epoxy intended to provide environmental protection and promote heat dissipation. The interior of S2 was not encapsulated. Additional specifications for these products are given in **Table 4-2**.

Table 4-2. Manufacturer's specifications for the multichannel drivers examined in this study.

Driver No.	Output Voltage Range (V)	Output Current Range (mA)	Max Output Power (W)	Driver Efficiency	PF	THD @ Max Load	Max Case Temp °C
DUT-S1	10-55	400-1,400	50	85%	>0.9	<10%	75
DUT-S2	27-54	100-1,100	40	85%	>0.95	<10%	75
DUT-S3	15-53	11-1,050	55	88%	>0.95	<20%	85

¹ The values in the table are given for 120 V operation only.

² Surge protection was measured with a ring wave.

Two samples of each DUT were programmed for operation at approximately 95% of the maximum specified current. Each sample was connected to an external LED load (as discussed in Section 3.1) and tested in the 7575 chamber for a total of 2,500 hours. The electrical performance of each driver was measured by Hubbell Lighting using a Chroma test stand when the drivers were new and after 2,500 hours of 7575 exposure. In addition, flicker measurements were acquired on the LED loads operated by the drivers throughout testing using the methods described in Section 3.3.3.

For the DUT-S1 samples, the electrical measurements revealed no significant difference relative to the control in output wattage, driver efficiency, PF, or dimming behavior after 2,500 hours of 7575 exposure. In addition, the photometric measurements indicated that the flicker percentage of these samples was less than 1%. The photometric flicker waveform was generally dc in character with a small square wave ripple having a flicker frequency exceeding 1,400 Hz both before and after 2,500 hours of exposure. This finding indicates that minimal degradation of the DUT-S1 samples occurred during the first 2,500 hours of AST testing.

For the DUT-S2 samples, the electrical measurements revealed a ~ 3-W decrease in output wattage for both samples, as shown in **Figure 4-8**. However, the driver efficiency and PF were the same before and after 2,500 hours of 7575 exposure. Because the change in output power was not accompanied by a decrease in efficiency, an increase in circuit impedance is not likely to be the root cause. Additional study is needed to identify the reason for this change. It should be noted that the decrease in output power may change the photometric performance of any luminaire incorporating this driver; however, this change in luminous flux is so small, at this point in testing, that it is unlikely to be noticed, unless the trend continues. Photometric measurements indicated that the flicker percentage of these samples was also less than 1% throughout testing. The photometric flicker waveform was generally dc in character with virtually no ripple both before and after 2,500 hours of exposure. This finding also indicates that minimal degradation of the DUT-S2 samples occurred during the first 2,500 hours of testing.

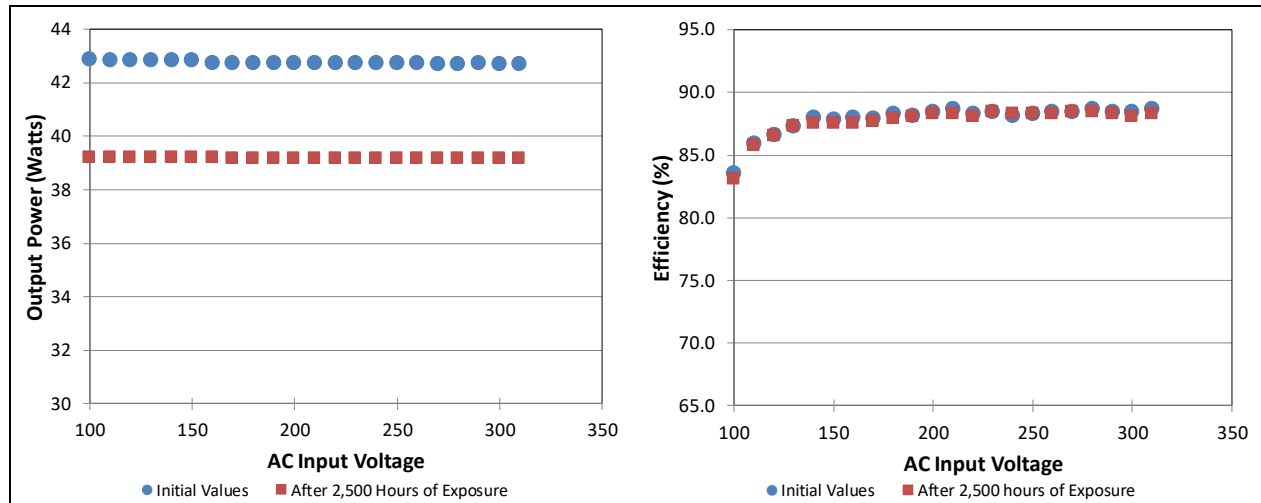


Figure 4-8. Output power and driver efficiency as a function of input voltage for DUT-S2.

For the DUT-S3 samples, the electrical measurements revealed unexpected increases in output wattage and efficiency for both samples after 2,500 hours of 7575 exposure, as shown in **Figure 4-9**. The increases in efficiency and power output after 7575 exposure were especially pronounced at ac input voltages of less than 200 V. The PF was unaffected by these changes and was the same before and after 7575 exposure. Another difference in this device was the 0–10 V dimming behavior, as shown in **Figure 4-10**. The root cause of this change is unknown at present. The higher power output will increase the luminous flux from any luminaire incorporating this driver. This change could ultimately increase the rate of lumen depreciation of any LEDs attached to this driver.

Photometric measurements demonstrated that a small sinusoidal ripple occurred in the light source driver of the DUT-S3 samples when operated at full power, and no significant difference was found between the control and 7575-exposed samples. The photometric flicker percentages of these samples were less than 1%, and the flicker frequency was 120 Hz both before and after 2,500 hours of exposure. Clearly, some changes occurred in this DUT, resulting in higher power output and greater efficiency. However, the flicker and PF were unaffected by these changes. The source of these changes is unknown at present but will be investigated further, along with the impact on the LED load.

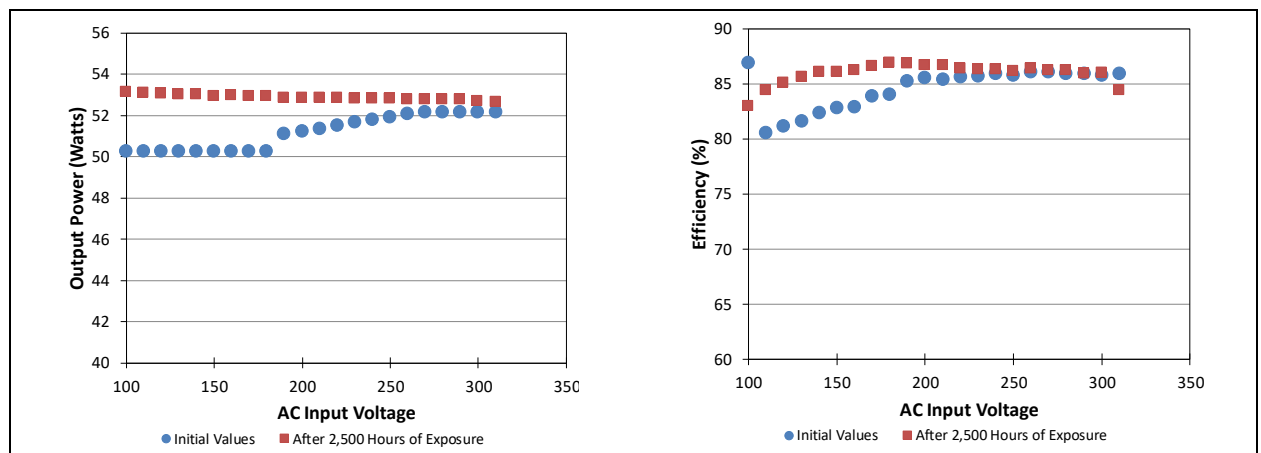


Figure 4-8. Output power and driver efficiency as a function of the input power for a DUT-S2 sample.

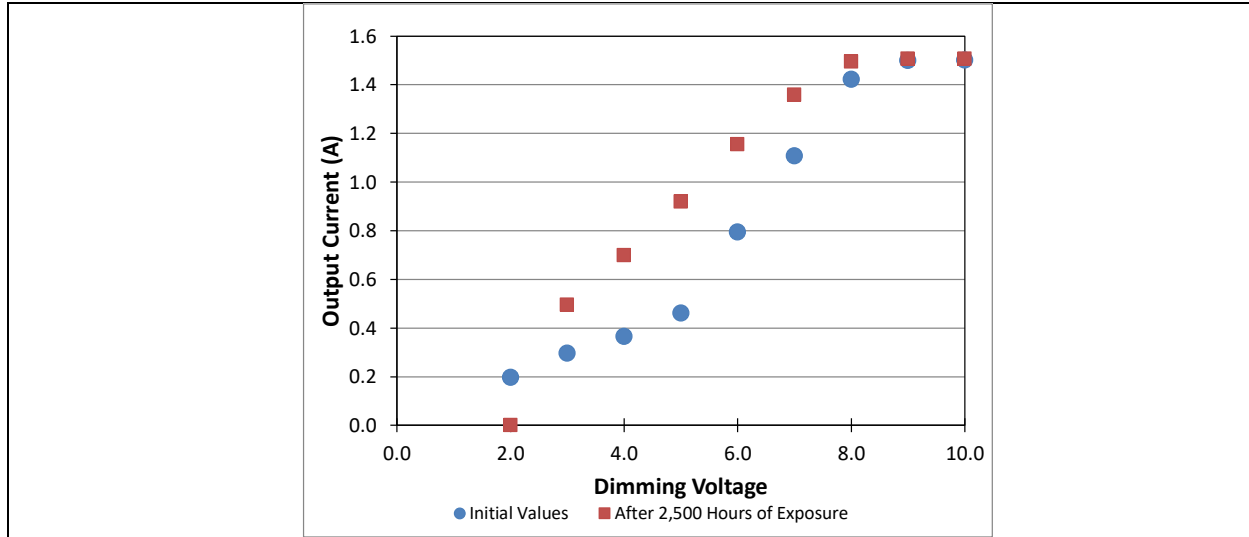


Figure 4–10. 0–10-V dimming characteristics of DUT-S3 before and after 7575 exposure.

4.3 Multichannel Drivers

Three different multichannel driver products, all capable of being used with TWL luminaires, were exposed to temperature and humidity environments for an extended time. All three products were Class 2 devices that can operate at input ac voltages between 120 V and 277 V, although in this work, they were operated at 120 V during 7575 exposure. The three products were rated for surge protection of 2 kV.

DUT-M1 is equipped with 0–10 V dimming and specified by the manufacturer to provide ingress protection (IP) equivalent to IP66. This driver has four channels, but only two were operated during these tests. The interior of DUT-M1 was fully encapsulated with a hard, black plastic. The LED loads used on the two channels of this driver were warm-white and cool-white LED modules, and the current required to operate these LEDs was approximately 90% of the specified load for each channel. The loads were mounted on aluminum heat sinks with separate dedicated warm-white and cool-white LED modules placed side by side on the heat sink. The same loads were used during the 7575 testing and all post-testing electrical and photometric characterizations.

The DUT-M2 and DUT-M3 products are both dimmable with DMX controls, and both are rated for use in dry and damp locations. The interiors of both products were unencapsulated, allowing easy access to the interior components. Both products also had four output channels; however, only two channels were used for product DUT-M2, whereas all four were used for DUT-M3. Equivalent loads were used for DUT-M2 and DUT-M3 although the load was distributed equally between two channels for DUT-M2 and four channels for DUT-M3. The warm-white and cool-white LED modules were housed on the same PCB with separate connections to the driver. Additional specifications for these products are given in **Table 4-3**.

Table 4-3. Manufacturer's specifications for the multichannel drivers examined in this study.

Driver No.	Output Voltage Range (V)	Output Current Range (mA)	Max Output Power (W)	Driver Efficiency	PF	THD @ Max Load	Max Case Temp °C
DUT-M1	30–54	700 typical	50	87%	>0.92	<20%	85
DUT-M2	2–55	200–1,050	50	89%	>0.9	<20%	85
DUT-M3	24	350–700	40		>0.9		90

¹ Values are given for 120 V operation only.

² Surge protection was measured with a ring wave.

4.3.1 DUT-M1

DUT-M1 is a four-channel driver intended for use in outdoor luminaires. The basic structure of the driver is a combination of PFC and inductor inductor capacitor (LLC) converter circuits in Stage 1 to produce dc power, which is then fed to separate buck inductors for each LED primary. Interactions between the control ICs and the different power conversion circuits help to control the overall dc output of the device. Only one sample of DUT-M1 was tested in 7575 because of its high-power output. Two additional samples were also tested in a more complex profile consisting of

- 250 hours of 7575;
- 250 hours of 8585; and
- 250 hours of power cycling in a closed chamber (DUT temperature varied between 35°C and 60°C).

This test was terminated when one of the DUT-M1 samples failed, although the other sample was still operational.

The TC readings from the DUT-M1 sample in 7575 are given in **Figure 4-11** at approximately the time when failure occurred. The TC records when device failure occurred because the electrical heating of the unit stopped when the part failed, and the temperature dropped to the chamber background level. Failure of the device did not actually occur during the 7575 test but happened afterwards when the unit was undergoing power cycling as the chamber temperature was cooling. In addition, failure of the DUT did not occur when the unit was first switched on but occurred roughly 35 minutes into the 2-hour power-on cycle. Similar observations were made for the unit that failed during 7575 exposure. Together, these findings suggest that cumulative damage from the AST likely caused the failure.

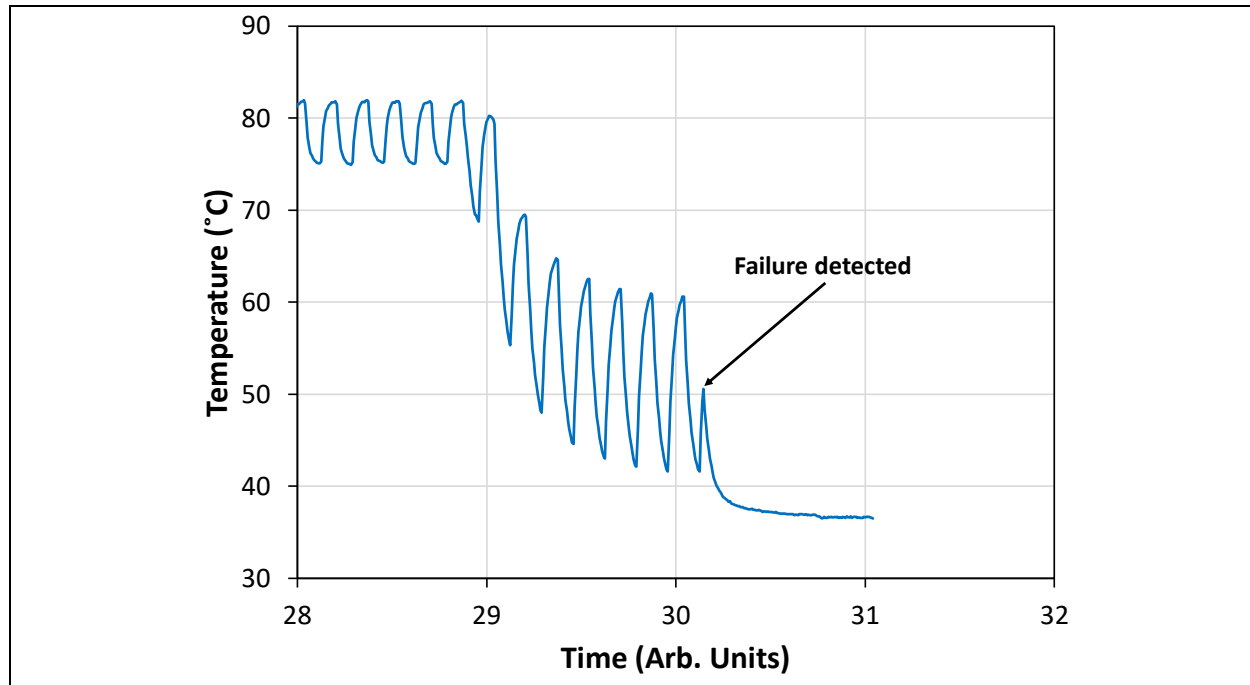


Figure 4-11. TC profile of the DUT-M1 sample in 7575 when failure occurred.

When device failure occurred, the power consumption and PF of the device dropped significantly, as shown in **Table 4-4**. However, the device continued to draw power, albeit at less than 10% of the initial level, which suggests that some of the circuits were still functioning. Thus, the device was still drawing 10 W of power, although no light was being produced. An analysis of the electrical characteristics of the device (performed by Hubbell Lighting) demonstrated that Circuit 1 and Circuit 2 (Figure 1-1) were performing as expected and that the failure likely occurred in Circuit 3. A subsequent analysis of the device by the manufacturer identified the failure of two film capacitors and the MOSFET in the resonant circuit of the LLC converter as the cause of failure. Virtually identical findings were obtained for the device that failed in the more complex temperature and humidity profile involving 8585 exposure.

Table 4-4. Change in the electrical properties of a DUT-M1 sample before and after 7575 exposure.

Test Condition	Input Current (A)	Input Power (W)	PF
Initial Value	1.17	140	0.99
Post-1,500-hour 7575 exposure	0.11	10.9	0.81

Photometric flicker measurements were taken on DUT-M1 before failure. The output waveform had a dominant dc characteristic with no discernable ripple waveform. The % flicker measured for the device was less than 0.5% until device failure occurred. Taken together, these findings indicate that minimal observable changes occurred in the device prior to catastrophic failure.

4.3.2 DUT-M2

DUT-M2 is a four-channel driver intended for indoor or outdoor use; in this study, only two of the channels were used. The basic structure of the driver comprises a combination of PFC and LLC converter circuits in Stage 1 to produce dc power, which is then fed to separate buck inductors for each stage. Two samples of DUT-M2 were tested, and both were still operational after 2,500 hours of exposure to a 7575 environment.

A comparison of the electrical characteristics (input volts, current, wattage, and inrush peak current; output volts, current, and wattage; and PF) of the control and sample devices revealed that little degradation of the sample device occurred during operation in the 7575 test conditions. All measurements were conducted at room temperature. There was, however, a difference in the inrush peak current for the sample device exposed to 7575 test conditions compared to the control device. As shown in **Figure 4-12**, the inrush peak current of the 7575-exposed device was consistently lower than that of the control device across the dimming range. The lower inrush peak current likely stemmed from higher impedance within the device, possibly because of higher capacitor equivalent series resistance, and suggests that some degradation occurred within the samples exposed to 7575. Electrical measurements also revealed slight differences in the input wattage and output wattage for each channel produced by the control and sample device; these differences represented a combination of slight variations in voltage and current.

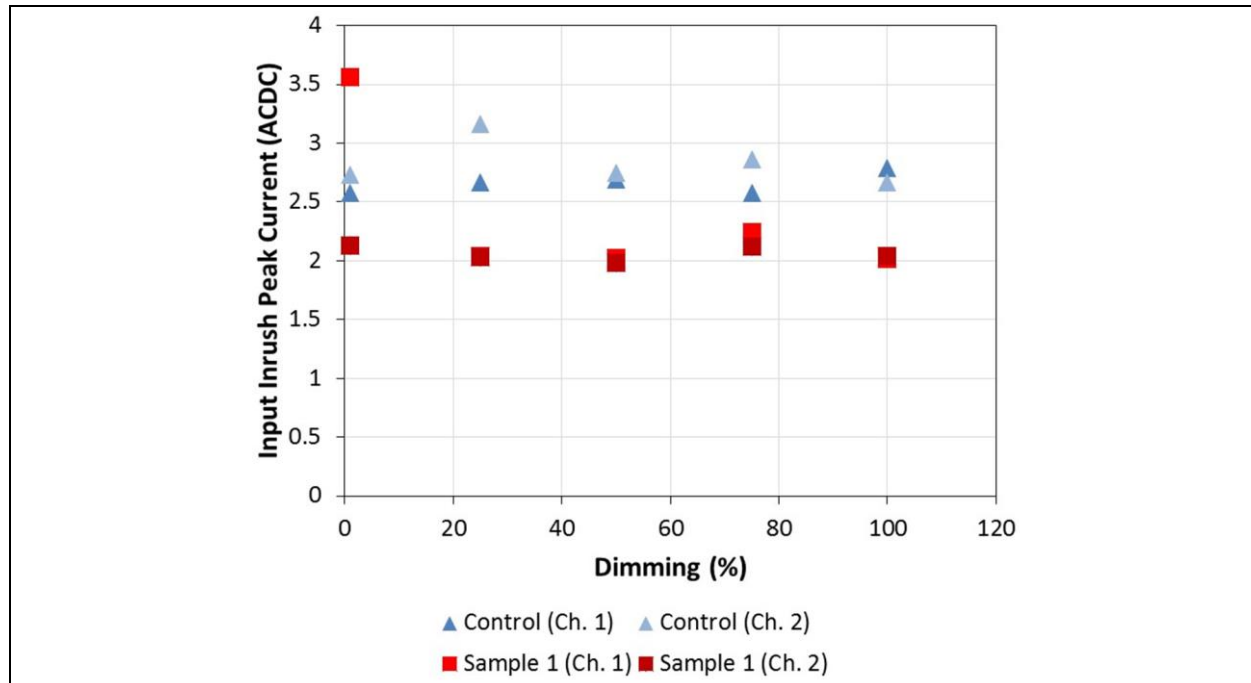


Figure 4-12. Inrush peak current comparisons of the control and sample DUT-M2 devices as a function of dimming percentage, showing higher inrush currents on the control device.

The dimming characteristics of the control and sample devices exposed to 7575 were also tested by connecting the drivers to a DMX dimmer. The driver efficiencies of the control and sample 1 are tabulated in **Table 4-5**. The slight variations in output current and voltage led to marginally lower sample device driver efficiencies for the samples exposed to 7575 (with an average efficiency difference of 0.33%) compared to the control device at all dimming levels except 25%. Finally, a significant difference was observed between the PFs of the control device and sample 1 at low dimming levels (**Figure 4-13**). This difference may be indicative of some degradation in the film capacitors in the circuit.

Table 4-5. Efficiencies of the control and sample 1 (post 2,500 hours of 7575 exposure) DUT-M2 drivers at various dimming levels

Dimming Level (%)	Control Device	Sample 1
100	85.17%	84.85%
75	79.15%	79.06%
50	66.87%	68.04%
25	35.26%	39.07%
1	4.98%	6.04%

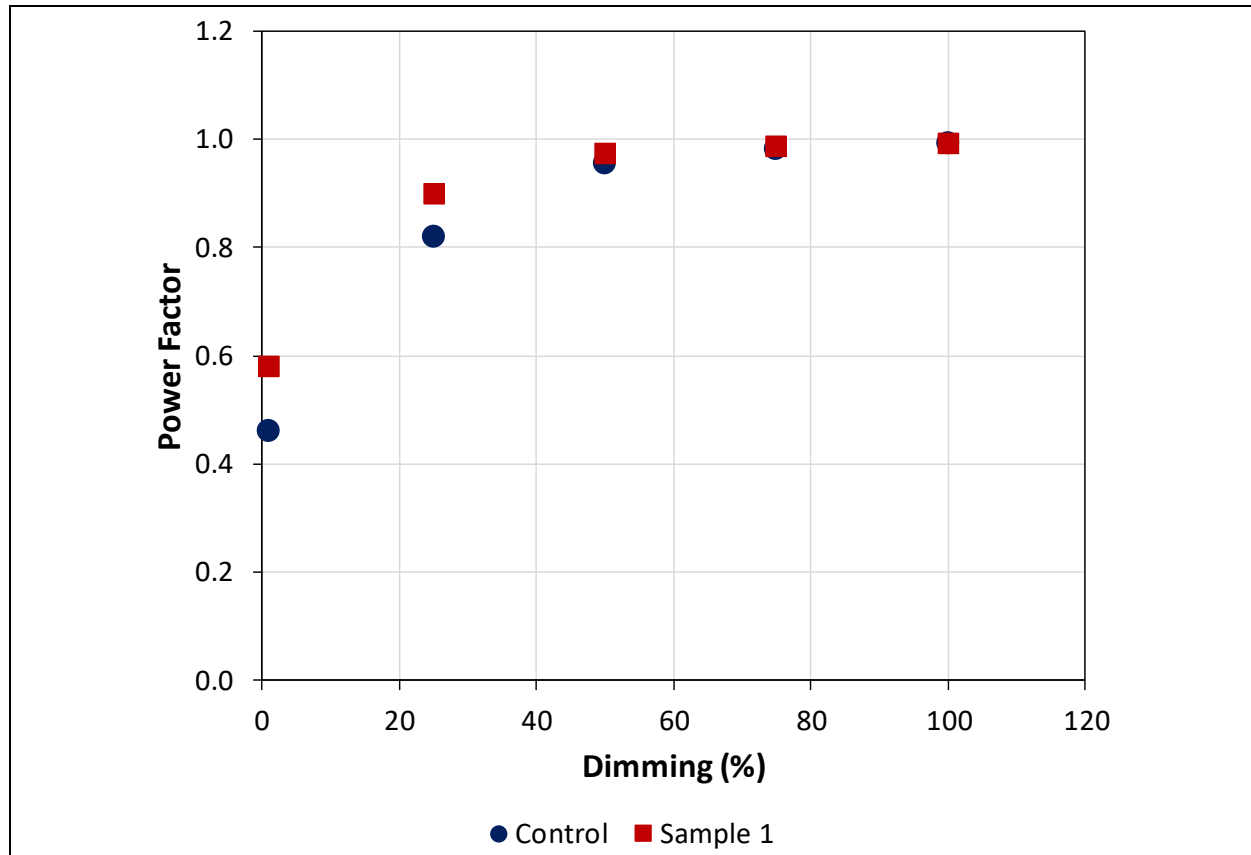


Figure 4-13. PF comparison of the control and sample DUT-M2 devices as a function of the dimming percentage

Flicker measurements were also collected from the DUT-M2 samples after 2,500 hours of exposure to 7575, and the results were compared to those of an unexposed control sample, as shown in **Figure 4-14**. DUT-M2 uses a hybrid flicker waveform that dynamically adjusts its amplitude and shape to achieve optimal efficiency. As a result, differences are likely to appear in each waveform at any point in time; however, the peak shape—mainly the rise and decay of the photometric flicker signal, especially at low dimming levels—provides insights into the potential degradation of the driver. As shown in Figure 4-14, the general shape of the photometric flicker waveform for this driver remained practically unchanged after 7575 exposure, although some differences were found in the amplitude because of the hybrid output waveform. This finding indicates that minimal degradation is detectable in the light output from the driver after 2,500 hours of 7575 exposure, despite the occurrence of subtle changes in the driver.

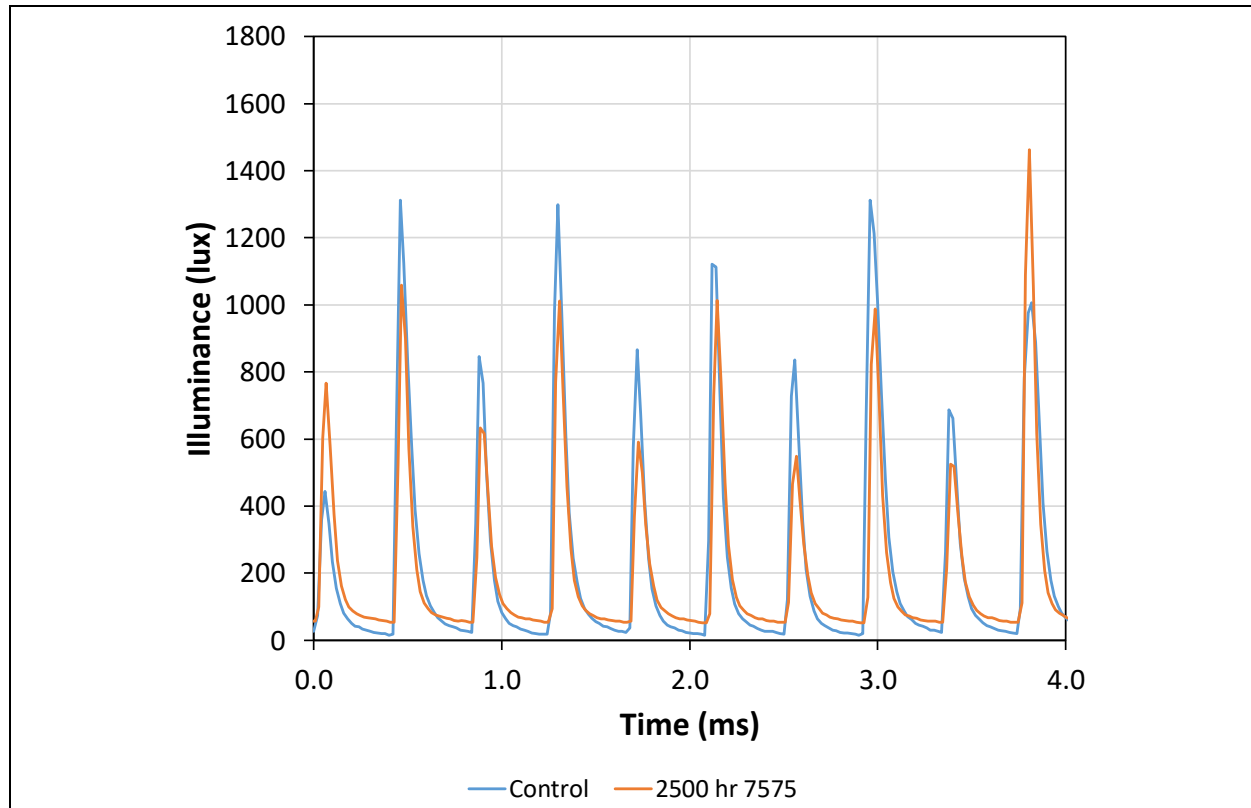


Figure 4-14. Comparison of the photometric flicker waveform, at 1% dimming, between a DUT-M2 sample after 2,500 hours of 7575 exposure and a control device.

4.3.3 DUT-M3

DUT-M3 is also a four-channel driver intended for indoor or outdoor use. All four channels were used during this test, and the LED load (equivalent to that for DUT-M2) was split between the four channels (instead of two for DUT-M2). The basic design of the driver is a flyback PFC converter for Stage 1 and separate buck circuits for Stage 2. In this device, the MOSFETs are integrated into the control IC, whereas separate MOSFETs and control ICs are used in the other drivers (Figure 1-3). Two samples of DUT-M3 were tested, and both samples were still operational after 2,500 hours of exposure to a 7575 environment.

Electrical measurements did not reveal a significant difference in the inrush peak current on any channel of the DUT-M3 devices. However, other electrical measurements (input volts, current, and wattage; output volts, current, and wattage; and PF) of the DUT-M3 devices suggested some differences in the device efficiency and PF of samples operated for 2,500 hours in the 7575 environment. Namely, the control device had slightly greater efficiency than the devices exposed to 7575 at all dimming levels (the average efficiency difference was 0.48%). The driver efficiencies of the control and sample 1 of DUT-M3 are tabulated in **Table 4-6**. The electrical measurements also showed slight differences between the PFs of the control device and sample 1 at low dimming levels (**Figure 4-15**). Overall, the electrical performance of DUT-M3 after 2,500 hours of 7575 exposure indicates minimal degradation and excellent consistency with the control device, despite the harsh test conditions.

Table 4-6. Efficiencies of the control and sample 1 (post 2,500 hours of 7575 exposure) DUT-M3 drivers at various dimming levels

Dimming Level (%)	Control Device	Sample 1
100	75.39%	74.67%
75	70.46%	69.85%
50	55.70%	55.27%
25	28.27%	28.33%
1	5.66%	5.71%

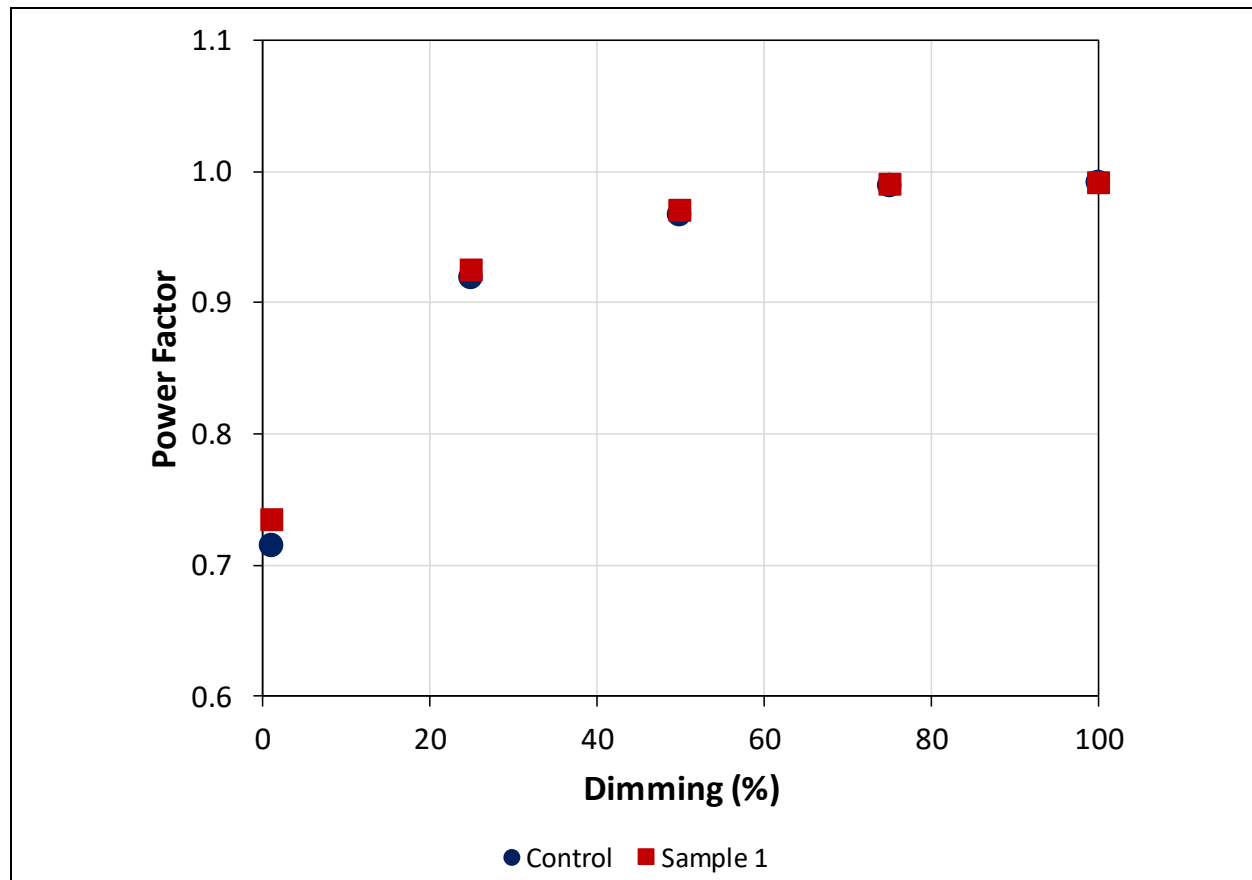


Figure 4-15. PF comparison of the control and sample DUT-M3 devices as a function of the dimming percentage

Flicker measurements were taken from the DUT-M3 samples after 2,500 hours of exposure to 7575, and the results were compared to those of an unexposed control sample. The results obtained at the 1% dimming level are shown in **Figure 4-16**. DUT-M3 uses a PWM waveform at low dimming levels; thus, the waveforms of the control and exposed samples are more comparable than for DUT-M2. As shown in Figure 4-16, the general shape of the photometric flicker waveform for this driver is virtually identical after 2,500 hours of 7575 exposure, indicating that no significant change occurred in the luminaire's light output properties, despite a small amount of degradation on the front end. Any variation in the pulse amplitude, frequency, and decay constant found by measuring the flicker of the LED load connected to the driver are likely the result of a combination of experimental variation and slight differences in the electrical properties between the two

drivers. This finding indicates that minimal change was detectable in the output from the driver after 2,500 hours of 7575 exposure, in agreement with the electrical measurements discussed above.

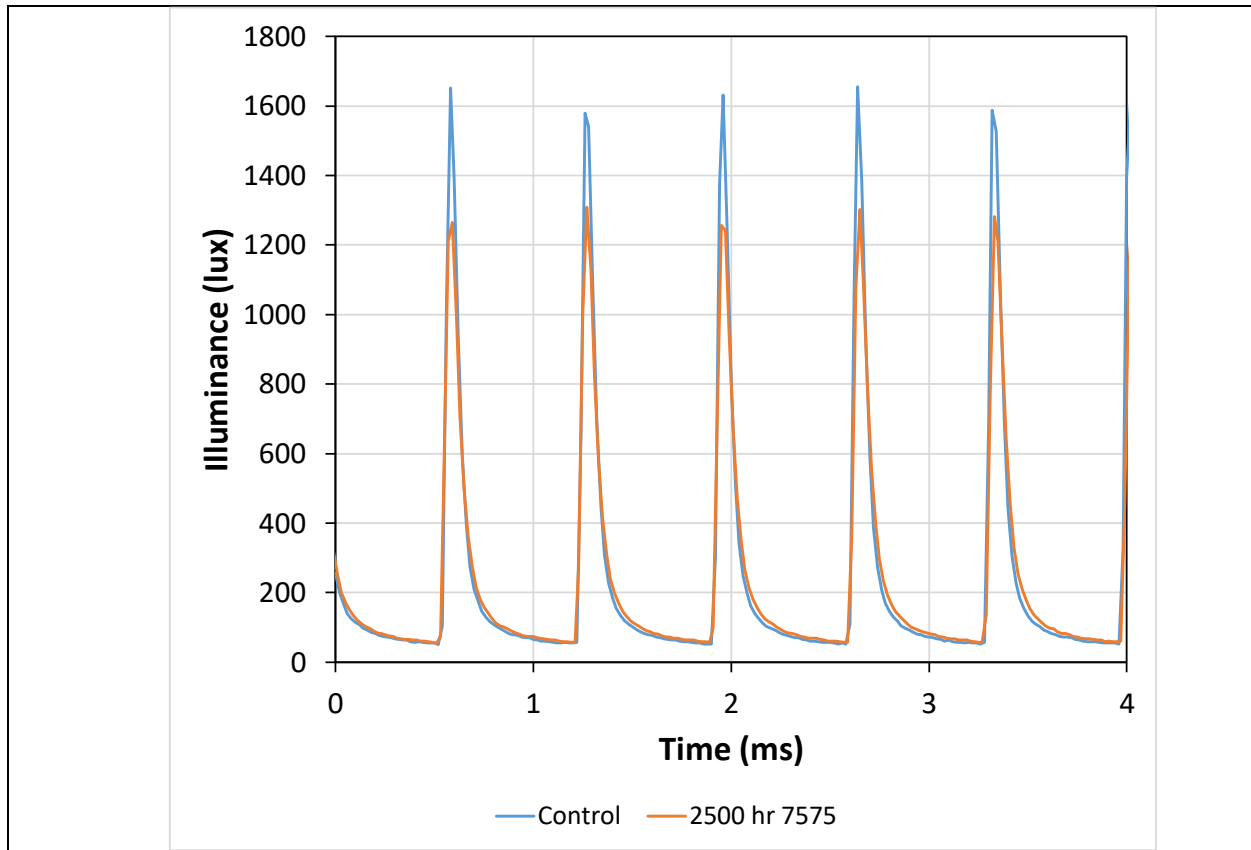


Figure 4–16. Comparison of the photometric flicker waveform, at 1% dimming, between a DUT-M3 sample after 2,500 hours of 7575 exposure and a control device.

5 Conclusions

Advanced light fixtures, such as TWL luminaires, require increased sophistication in the LED driver to operate the multiple LED primaries used in these devices. Such drivers must provide separate dc outputs for each LED primary, which requires that each primary have a dedicated dc supply channel. In addition, each driver typically contains two power conversion stages (i.e., a two-stage driver) to provide high PF and minimal THD. This study examined how this added functionality in the driver impacted the robustness of the device and whether degradation in the front end of the circuit would impact the quality of light produced by the LED load.

AST exposure studies, performed in a 7575 environment, were conducted on six different LED driver products that could be used in luminaires, including TWL luminaires. The tested products consisted of three different two-stage single-channel driver products and three different two-stage multichannel driver products. The AST study demonstrated that the robustness of the stand-alone drivers was excellent. Only two out of 12 products (16.7%) failed during the first 2,500 hours of testing. This failure rate was significantly better than that observed for 6" SSL downlights in the same test, where 38% of the test population failed in a comparable period. The two failed devices were samples of the same product, and in both instances, failure was traced to the film capacitors and the MOSFET on the LLC resonator circuit.

The surviving parts were thoroughly characterized both electrically and photometrically to understand any changes that occurred during the accelerated test. Half of the surviving products had a small decrease in one or more electrical parameters, while the other half had a slight increase. The measured parametric changes included power output and inrush current. However, no significant change in important photometric parameters (e.g., luminous flux and flicker) or electrical parameters (e.g., PF and THD) was measured for these devices, even after 2,500 hours of 7575 exposure. This finding is especially important because significant changes in luminous flux output and flicker may be recognized by the end-user and considered failure. PF and THD are less likely to be directly noticed by the end-user. However, changes in these electrical properties could lead to future problems in the driver or other devices connected to the branch circuit.

References

1. Davis, J. L., Mills, K., Yaga, R., Johnson, C., & Young, J. (2017). Assessing the reliability of electrical drivers used in LED-based lighting devices. In W. D. van Driel, X. Fan, & G. Q. Zhang (Eds.), *Solid state lighting reliability part 2: Components to systems*. Springer.
2. Winder, S. (2008). *Power supplies for LED driving*. Burlington, MA: Newnes.
3. Next Generation Lighting Industry Alliance, LED Systems Reliability Consortium. (2014). *LED luminaire lifetime: Recommendations for testing and reporting, Third Edition*. Washington, D.C.: September 2014. Available from https://energy.gov/sites/prod/files/2015/01/f19/led_luminaire_lifetime_guide_sept2014.pdf.
4. Pacific Northwest National Laboratory. (2016). *CALiPER Report 23: Photometric testing of white-tunable LED luminaires*. January 2016. Report Number PNNL- 24595. Washington, D.C.: DOE, 2016. Available from https://energy.gov/sites/prod/files/2016/01/f28/caliper_23_white-tunable-led-luminaires.pdf.
5. Pacific Northwest National Laboratory. (2014). *CALiPER Retail Lamps Study 3.1: Dimming, flicker, and power quality characteristics of LED A lamps. Report Number PNNL-SA-23944*. Washington, D.C.: DOE, 2014. Available from https://energy.gov/sites/prod/files/2015/01/f19/caliper_retail-study_3-1.pdf.
6. Pacific Northwest National Laboratory. (2014). *CALiPER Report 20.3: Robustness of LED PAR38 lamps. Report Number PNNL-SA-23971*. Washington, D.C.: DOE, 2014. Available from https://energy.gov/sites/prod/files/2015/02/f19/caliper_20-3_par38.pdf.
7. Davis, J. L., Young, J., & Royer, M. (2016). *CALiPER Report 20.5: Chromaticity shift modes of LED PAR38 lamps operated in steady-state conditions*. Report Number PNNL-25201. Washington, D.C.: DOE, 2016. Available from https://energy.gov/sites/prod/files/2016/03/f30/caliper_20-5_par38.pdf.
8. RTI International. (2013). *Hammer testing findings for solid-state lighting luminaires*. (prepared for the U.S Department of Energy) 2013, December. Available from https://www1.eere.energy.gov/buildings/publications/pdfs/ssl/hammer-testing_Dec2013.pdf.
9. Clark, T. (2016, November 21). Future-proof tunable white lighting is a smart choice for classrooms. *LEDs Magazine*, 13. <http://www.ledsmagazine.com/articles/print/volume-13/issue-9/features/tunable-lighting/future-proof-tunable-white-lighting-is-a-smart-choice-for-classrooms>
10. Davis, J. L., Mills, K., Hensley, E., Clark, T., & Smith, A. (2017). *Luminaires for advanced lighting in education. Final report of DOE project DE-EE0007081*. Washington, D.C.: DOE, 2017. DOI: 10.2172/1367149. Available at <https://www.osti.gov/scitech/servlets/purl/1367149>.
11. Davis, R. G., & Wilkerson, A. (2017). *Tuning the light in classrooms: Evaluating trial LED lighting systems in three classrooms at the Carrollton-Farmers Branch Independent School District in Carrollton, TX. Report Number PNNL-26812*. Washington, D.C.: DOE, 2017. Available from https://energy.gov/sites/prod/files/2017/10/f37/2017_gateway_tuning-classroom_0.pdf.
12. Davis, R. G., Wilkerson, A. M., Samla, C., & Bisbee, D. (2016). *Tuning the light in senior care: Evaluating a trial LED lighting system at the ACC Care Center in Sacramento, CA. Report Number PNNL-25680*. Washington, D.C.: DOE, 2016. Available from https://www.energy.gov/sites/prod/files/2016/09/f33/2016_gateway-acc.pdf.

13. Wilkerson, A., Davis, R. G., & Clark, E. (2017). *Tuning hospital lighting: Evaluating tunable LED lighting at the Swedish Hospital Behavioral Health Unit in Seattle. Report Number 26606.* Washington, D.C.: DOE, 2017. Available from https://www.energy.gov/sites/prod/files/2017/08/f36/2017_gateway_swedish-tuning-led_0.pdf.
14. Lutron. (2017). *Application Note #579: Color tuning with Lutron controls, Revision D.* Available from <http://www.lutron.com/TechnicalDocumentLibrary/048579.pdf>.
15. Cypress Semiconductor. (2015). *Specification sheet for CY8CLED04D01 PowerPSoC Intelligent LED Driver.* Available from <http://www.cypress.com/file/126871/download>.
16. Davis, J. L., & Mills, K. (2017). *System reliability model for solid-state lighting (SSL) luminaires. Final report of DOE project DE-EE0005124.* Washington, DC: DOE.
17. Perrin, T. E., Brown, C. C., Poplawski, M. E., & Miller, N. J. *Characterizing photometric flicker. Report Number PNNL-25135.* Washington, D.C.: DOE, 2017. Available from <https://energy.gov/sites/prod/files/2016/03/f30/characterizing-photometric-flicker.pdf>.
18. Athalye, P., Harris, M., & Negley, G. (2012). *A two-stage LED driver for high performance high-voltage LED fixtures.* Presented at the 2012 27th Annual IEEE Applied Power Electronics Conference and Exposition, Orlando, FL. DOI: [10.1109/APEC.2012.6166157](https://doi.org/10.1109/APEC.2012.6166157).

Appendix A

Table Appendix A-1. Identifying information for the samples included in this report

Brand	Model	Type	Max Power Rating	Mass	ID Number
LEDNovation	LEDH-A19-60-1-27D-IO-E	A19 lamp with hybrid LED light source	9.4 W	90 g	13-RT08 ^a
Cree	LRP38-10L-30K-12	PAR38 lamp with hybrid LED light source	13.5 W	541 g	12-67 ^b
Cree	LR6C DR1000 XP	6" downlight with hybrid LED light source	12 W	1,136 g	Luminaire A
Osram	Optotronic OT50W/PRG1400C/UNV/DIM/L	Single channel driver	50 W	279 g	DUT-S1
Philips Advance	XI040C110V054BPT1	Single channel driver	40 W	316 g	DUT-S2
Everfine	D15CC55UNVT-C	Single channel driver	55 W	473 g	DUT-S3
LG	LLP 150W 0.7 A	Multichannel driver	150 W	1,178 g	DUT-M1

A See reference [5].

B See reference [6, 7].

C See reference [8].

U.S. DEPARTMENT OF
ENERGY

Office of
**ENERGY EFFICIENCY &
RENEWABLE ENERGY**

For more information, visit:
energy.gov/eere/ssl

DOE/EE-1747 • February 2018 (Revised June 2018)